

2609
ORNL-6262

DOE/NASA/4148-1
NASA CR-175019

Joining of Ceramics for Advanced Heavy-Duty Diesels

(NASA-CR-175019) JOINING OF CERAMICS FOR
ADVANCED HEAVY-DUTY DIESELS (Oak Ridge
National Lab.) 63 p EC A04/MF A01 CSCL 11C

N86-24846

Unclas
G3/27 43380

A. J. Moorhead and H. Keating
Metals and Ceramics Division
Oak Ridge National Laboratory

March 1986

Prepared for
NATIONAL AERONAUTICS AND SPACE ADMINISTRATION
Lewis Research Center

for
U.S. DEPARTMENT OF ENERGY
Conservation and Renewable Energy
Office of Transportation Systems
Under Interagency Agreement 40-1254-82

ORNL-6262
Distribution
Category UC-95

METALS AND CERAMICS DIVISION

JOINING OF CERAMICS FOR ADVANCED HEAVY-DUTY DIESELS

A. J. Moorhead and H. Keating

Date Published — March 1986

Prepared by the
OAK RIDGE NATIONAL LABORATORY
Oak Ridge, Tennessee 37831
operated by
MARTIN MARIETTA ENERGY SYSTEMS, INC.
for the
U.S. DEPARTMENT OF ENERGY
under Contract No. DE-AC05-84OR21400

591
EA 789470

CONTENTS

ABSTRACT 1
INTRODUCTION 1
BRAZING THEORY AND BACKGROUND 3
 THEORY OF WETTING AND ADHERENCE 7
 RATIONALE FOR A FRACTURE MECHANICS APPROACH TO BRAZE JOINT
 EVALUATION 10
EXPERIMENTAL PROCEDURE AND EQUIPMENT 12
 SESSILE-DROP WETTABILITY 12
 SESSILE-DROP SPECIMEN CHARACTERIZATION 13
 FLEXURAL STRENGTH MEASUREMENT OF BRAZED JOINTS 15
 CRITICAL FRACTURE TOUGHNESS, K_{Ic} , OF BRAZEMENTS 16
 SHEAR STRENGTH OF CERAMIC-METAL BRAZEMENTS 18
MATERIALS 20
 STRUCTURAL CERAMICS 20
 STRUCTURAL METALS 21
 EXPERIMENTAL FILLER METALS 25
EXPERIMENTAL RESULTS 27
 SILVER AND COPPER BASED SYSTEM 28
 COPPER AND GOLD BASED SYSTEMS 31
 FRACTURE TOUGHNESS OF THE BRAZEMENTS 35
 SHEAR STRENGTH OF THE CERAMIC-METAL JOINTS 36
DISCUSSION OF RESULTS 36
 VARIABILITY IN BOND STRENGTH DATA 36
 EFFECT OF ACTIVE FILLER METALS ON PSZ 42
 COMPARISON OF FILLER METAL WETTING ON MgO- AND
 Y₂O₃-STABILIZED ZIRCONIAS 45
 EFFECT OF 1000°C BRAZING CYCLE ON NODULAR CAST IRON 47
SUMMARY AND CONCLUSIONS 47
REFERENCES 50

PRECEDING PAGE BLANK NOT FILMED

JOINING OF CERAMICS FOR ADVANCED HEAVY-DUTY DIESELS*

A. J. Moorhead and H. Keating

ABSTRACT

The wettability and adherence in vacuum of a series of metal alloys on several oxide ceramics were investigated with the goal of identifying those compositions suitable as filler metals for direct brazing of ceramics in uncooled diesel engine applications. Wetting behavior was determined by the sessile-drop technique. Adherence was measured by several tests including sessile-drop shear, flexure strength of ceramics brazed in a butt-joint configuration, fracture toughness using a composite double cantilever beam specimen, and, in the case of ceramic-metal brazements, by a bar/pad shear test. Compositions were identified in both the Cu-Ag-Ti and Cu-Au-Ti ternary systems that wet and strongly adhered to high-purity aluminas, partially stabilized zirconia ceramics, and alumina reinforced with SiC whiskers. Excellent flexural strengths, at temperatures up to 600°C, of brazements containing these filler metals indicate that these materials are good candidates for use in advanced heavy-duty diesel engines. They have the advantage over competing systems of not requiring that the ceramic be metallized before brazing.

INTRODUCTION

Although monolithic ceramic materials have been widely used in the past in nonstructural applications such as electrical insulators, crucibles, microwave windows, and pump and valve components for the chemical industry, it has been only in recent times that major efforts have been made to use ceramics in structural applications where significant tensile or multiaxial stresses are imposed over a range of temperatures. The major impetus for most of this interest over the past decade is economics — as fuel costs have increased so has the need for increased efficiency in a multitude of energy conversion processes.

*Research sponsored by the National Aeronautics and Space Administration, Lewis Research Center, Heavy Duty Diesel Engine Technology Program, under Interagency Agreement 40-1254-82, and the U.S. Department of Energy, Office of Transportation Systems, under contract DE-AC05-84OR21400 with Martin Marietta Energy Systems, Inc.

Ceramic materials show considerable promise for use in advanced heat engines. The impetus to increase engine efficiency and performance has led to continuing improvements in material use temperatures. A number of automotive manufacturers are working to develop a more efficient diesel engine for cars or trucks that eliminates the need for power-consuming cooling requirements by using structural ceramics in the combustion chamber — cylinder, piston cap, and valve plate as shown in Fig. 1. There is also interest in ceramics as wear pads attached to components such as valve rocker arms and push rods. The use of petroleum materials could be reduced even further through use of high-temperature ceramic bearings and solid lubricants.

ORNL-DWG 84-9396

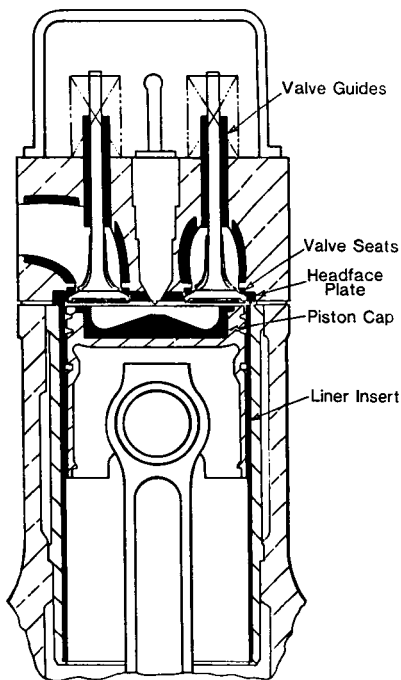


Fig. 1. Cross section of combustion chamber of prototype uncooled diesel engine with ceramic components identified.

The NASA Lewis Research Center (LeRC) was assigned project management responsibility for the Heavy Duty Transport Technology Project by the U.S. Department of Energy. The major thrust of this program is to support long-term, high-risk, but potentially high-payoff, research and development on promising conservation technologies that are related to the heavy-duty transport sector but are unlikely to be undertaken by the private sector

alone. To that end, LeRC issued an Applications Notice describing the areas of interest and invited unsolicited proposals in those areas. Oak Ridge National Laboratory (ORNL) submitted a proposal, which was accepted by LeRC. The proposal was for a two-year study with the first-year effort to emphasize the development of brazing filler metals that would wet and adhere to typical insulating ceramics such as partially stabilized zirconia (PSZ) and alumina, which are being considered for the uncooled diesel, and also nodular cast iron, which is a principal structural metal for that engine. The first year was to include the completion of short-term, room-temperature mechanical property tests on ceramic-ceramic and ceramic-metal brazements. During the second year the research was to focus on longer-term and elevated-temperature property tests as well as brazing studies on ceramic-matrix composites that were being developed at ORNL as potential substitutes for PSZ. The program was terminated after the first year because it had been decided that this ceramic brazing research should be funded through the Ceramic Technology for Advanced Heat Engines Project being managed by ORNL. Because of a shortage of manpower and delays in equipment development, the first-year funds provided by NASA-LeRC were spent over a period of 21 months, and it is that work which is reported here. Because more generic ceramic brazing research was also being funded simultaneously under the Energy Conversion and Utilization Technologies (ECUT) Program, both programs were able to benefit through shared funding for equipment and technique development.

BRAZING THEORY AND BACKGROUND

At least three techniques appear to have some promise for joining of ceramics for high-performance applications: (1) mechanical joining, (2) brazing, and (3) diffusion welding. We concluded, on the basis of careful consideration of the advantages and disadvantages of each technique, that brazing had the most potential for meeting the ceramic joining requirements in heat engines such as the advanced heavy-duty diesel or advanced gas turbine, in high-temperature heat exchangers, and in a host of other industrial applications of ceramics.

However, brazing of ceramics is considerably more difficult than brazing of metals. Most commercially available brazing filler metals (sometimes referred to as "braze alloys") do not wet ceramic materials. This problem is generally overcome by first applying a metallic coating to the ceramic substrate and then brazing to this coating with a conventional filler metal. The large commercial ceramic-to-metal seal industry and many electronic applications are based on one of these indirect techniques — the "moly-manganese" process.¹ In another indirect brazing technique the ceramic is coated with an active metal such as titanium either from the thermal decomposition of a hydride² or by ion plating.^{3,4}

Other researchers have developed filler metals (with active-metal alloying additions) that wet some ceramic materials directly without the need for precoating.^{5,6} Direct brazing avoids the development and application of what is, in many cases, a very sophisticated coating or metallizing treatment. The inclusion of the active metal within the filler metal protects it from oxidation during storage or while brazing — a problem with active-metal coatings. Also the bond strength and corrosion resistance of a coating do not have to be of concern. Filler metals used for direct brazing (as those used to braze precoated ceramics) generally do not have the oxidation resistance of many high-purity ceramics at their maximum service temperatures. Through judicious design, a braze joint may be located in a less severe environment. For example, it has been predicted that in the uncooled diesel engine the temperature at the interface between ceramic piston cap and metallic piston will be about 350°C as compared with 1000°C on the top surface of the cap.

The wetting and adhesion of a metal (the brazing filler metal) on a ceramic substrate are affected by a number of complex, interrelated factors — chemical, mechanical, or geometrical. Chemical factors include the chemical activities of the various filler metal constituents; the tendency, or lack thereof, to form stable oxides; and the rate and products of any interfacial reactions. Mechanical factors that must be considered are the relative thermal expansions and bulk strengths of the filler metal and substrate, and the surface roughness of the substrate. Some typical properties of structural ceramics and metals are given in Table 1 for

Table 1. Typical physical and mechanical properties of commercial structural ceramics and common metal alloys

Property	Al ₂ O ₃	PSZ ^a	α-SiC	Si ₃ N ₄	4340 steel	Ductile iron	6061-T651 aluminum	304 steel
Fracture strength ^b (MPa)	350	600-700	460	650	1200	690	290	590
Fracture toughness (MPa·m ^{1/2})	4	6-14	4	4.5	116	30	30	450 ^c
Coefficient of thermal expansion (× 10 ⁶ /°C)	8	>10 ^d	4	3	11	12	25	20
Modulus of elasticity (GPa)	405	205	405	320	205	165	69	200

^aPartially stabilized zirconia.

^bFour-point-bend flexural strength for ceramics, ultimate tensile strength for metals.

^cCalculated equivalent of J_{Ic} .

^dTemperature range over which thermal expansion hysteresis occurs. Depends upon composition and microstructure of the PSZ.

comparison. Of course geometrical factors such as thickness, area, and shape of the interface and relative positioning of members are always important. As will be seen later, each of these factors contributes to either the success or failure of a given brazement.

The objective of this research was to develop brazing filler metals that would wet and strongly bond to the structural ceramics and metals being considered for the advanced heavy-duty diesel engine without the need for precoating of the ceramic to promote adherence. Our goal was to achieve brazing temperatures sufficiently low that the other potential structural components would not be damaged by the thermal processing cycle, with filler metals that would have "adequate" strength and oxidation resistance in air at service temperatures of about 350°C. We did not have specific guidelines as to what "adequate" strength really was, but there was some information from representatives of Cummins Engine Company, Inc., that a room-temperature shear strength of at least 100 MPa would be required in the crucial piston cap to piston brazement, and that is the value we tried to meet. The ceramic materials included in this study were: (1) an MgO-stabilized partially stabilized zirconia* (PSZ); (2) Y₂O₃-stabilized tetragonal zirconia polycrystalline (TZP) ceramic;† (3) three high-purity, high-density commercial aluminas — Coors‡ AD-99 and AD-998 and Degussit AL-23;§§ and (4) a SiC-whisker-reinforced alumina composite under development at ORNL.⁷ In the ceramic-to-metal brazements, the metals included a nodular cast iron,†† type 446 stainless steel, and titanium. The latter metals were chosen as potential transition materials to aid in accommodating mismatches in coefficients of thermal expansion of the ceramics and the cast iron.

Our approach was to select simple binary metal systems that had relatively low melting temperatures and then add varying amounts of titanium

*Nilsen MS Grade.

†NGK Ceramics, Z-191 Grade.

‡Coors Porcelain Co., Golden, Colo.

§§Degussa, Federal Republic of Germany.

††Izumi piston material.

to promote wetting and bonding to the oxide ceramics. Binary systems were chosen that had previously been used commercially for brazing of metals. Although other reactive metals have been used in some direct brazing filler metals, titanium is thought to have the most universally beneficial effect and so it was used throughout this study. The effect of titanium in promoting wetting of oxide ceramics is not yet fully understood, but some plausible reasons will be discussed later in the section titled Experimental Filler Metals.

After melting of small amounts of the experimental filler metals, wetting and bonding studies were conducted on small ceramic pads. Most of the effort in this program went into ceramic brazing because that aspect of the joining problem is much more difficult than brazing of a metal. We believed it was highly likely that any filler metal that would bond to an oxide ceramic would also adhere to a metal. Adherence of the brazes was determined by room-temperature shear tests, room- and elevated-temperature flexure tests, and fracture toughness tests.

THEORY OF WETTING AND ADHERENCE

As can be seen in Fig. 2, the shape of a drop of liquid (in our case, molten filler metal) on a solid surface (ceramic in this case) is determined by gravity and interacting forces of solid-liquid interfacial energy (γ_{SL}), solid-vapor interfacial energy (γ_{SV}), and liquid surface tension (γ_{LV}). This balance of interfacial tensions is characterized at equilibrium (with reference to Fig. 2) by the Young equation:

$$\cos\theta = \frac{\gamma_{SV} - \gamma_{SL}}{\gamma_{LV}} \quad (1)$$

The angle between the solid surface and the tangent to the liquid surface at the contact point or "contact angle θ " may vary from 0 to 180°. If γ_{SL} is high, the liquid tends to form a ball having a small interface area. If γ_{SV} is relatively high, the drop tends to spread. The effect of the

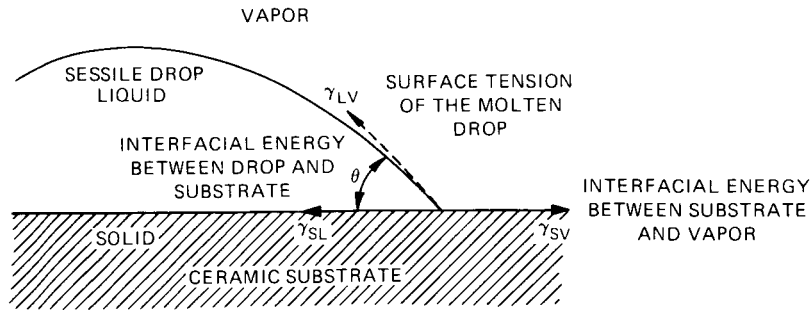


Fig. 2. Surface energy forces acting on a sessile drop.

liquid-vapor interfacial energy (surface tension) is not as straightforward. If only the liquid surface energy is decreased, the contact angle decreases (i.e., wetting is increased) for initially wetting drops ($\theta < 90^\circ$), but it increases for initially nonwetting drops ($\theta > 90^\circ$) as illustrated in Fig. 3. Thus, improved wetting always results when the solid-liquid interfacial energy (γ_{SL}) is decreased, and it may be obtained in some cases by decreasing γ_{LV} . A contact angle θ of 90° is assumed to be the boundary between "nonwetting" ($\theta > 90^\circ$, liquid depression in a capillary) and "wetting" ($\theta < 90^\circ$, liquid elevation in a capillary). From a practical brazing standpoint a contact angle of about 70° has been found to be satisfactory.⁸

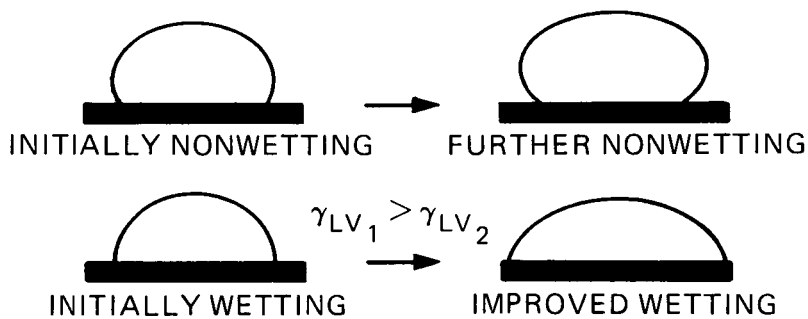


Fig. 3. Effect on contact angle of decreasing liquid surface tension (γ_{LV}) in the case of an initially nonwetting drop (upper) and initially wetting drop (lower).

The associated adhesive energy or work of adhesion (W_A) between the sessile drop and substrate that represents the free energy change for separation of a unit area of interface into a liquid and a solid surface can be expressed by the Dupre equation as:

$$W_A = \gamma_{SV} + \gamma_{LV} - \gamma_{SL} \quad (2)$$

or combined with the Young equation as

$$W_A = \gamma_{LV} (1 + \cos\theta) \quad (3)$$

The work of adhesion gives some indication of the adherence of the drop to the substrate, but it does not necessarily predict the adherence of the solidified drop.

The assumptions in the above equations of equilibrium conditions and the absence of any diffusion or reaction at the contact interface are seldom valid, particularly in our work in which we are trying to promote adherence by the addition of active metals to our brazing filler metals. As illustrated in Fig. 4, typically what originally was a two-phase system evolves into a three-phase system. The third or interface phase can result from the reaction with impurities at the interface, the diffusion of elements to the interface leading to reactions, or the alloying of components of phases (1) and (2) at the interface.⁹ Also, reaction between the molten metal and ceramic substrate and the subsequent solidification of the drop can create defects and stress concentrations at the metal-ceramic interface that will control the fracture mechanism. Because of these uncertainties over the validity of the work-of-adhesion values from sessile-drop experiments in the reactive systems being used in our work (and in the work of Ritter and Burton who found no correlations between thermodynamic work of adhesion and practical adhesive strength),¹⁰ we used this technique simply as a convenient means for determining the approximate solidus temperature of a filler metal and for observing the effect of time, temperature, and atmosphere on the wettability (as determined by contact angle measurements) of these alloys on ceramic substrates. We then measured the adhesive strength of the bonds directly by a mechanical test discussed in a later section.

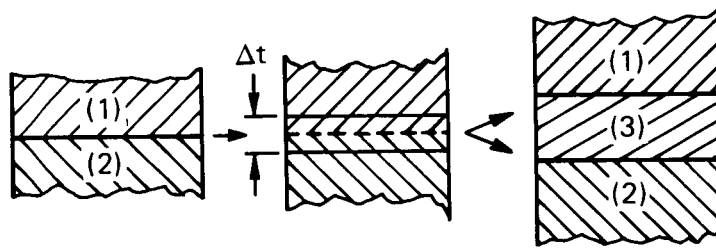


Fig. 4. The evolution of a two-phase equilibrium sessile-drop system into a three-phase system, where Δt is the interface phase thickness.

RATIONALE FOR A FRACTURE MECHANICS APPROACH TO BRAZE JOINT EVALUATION

The traditional engineering approach to design of fail-safe structures has been the use of conservative nominal shear or tensile strengths of the braze joint. However, the strength values achieved are strongly influenced by the existence of a critical defect or flaw. The variability in strengths is a measure of flaw size and not the intrinsic bond strength. Therefore, the evaluation of fracture mechanics has become increasingly important to the designer, and methods of analytically describing the resistance of a material to fracture have been developed. Braze joints are generally designed on the basis of shear strength data. However, we contend that many joints are loaded in tension at least part of their lives, so it is important to know how they behave under those conditions. Braze joints by their nature contain flaws that under crack-opening (tensile) conditions could cause failure. Along with the measurement of shear- and flexural-strength properties of our brazements, we therefore used a fracture mechanics test to study the fracture behavior of braze joints between ceramic base materials.

Because the failure stress of a ceramic brazement is a function of both the flaw size distribution (e.g., unbonded interfacial areas or voids) and the true adherence, a strength test by itself cannot determine the cause of failure, i.e., whether the value is the result of a large flaw or poor adherence. Nondestructive examination or post-failure analysis may allow the flaw size to be determined, and thus give a more comprehensive evaluation, but to observe this distinction in such systems is difficult

at best. On the other hand, fracture mechanics can be used to determine adherence in a fashion similar to that used to describe fracture in bulk brittle materials. Either the stress intensity factor in mode I (tensile) loading (K_I) or strain energy release rate G_I (where G_I is twice the fracture energy required to separate the interface) can be used to determine the ease of crack propagation either along an interface (adhesive failure) or in an adjacent phase (cohesive failure). Adherence is thus described in terms of the ability of the total brazement to resist fracture, which serves not only as a tool to examine adherence mechanisms but also as an important design tool.

The application of fracture mechanics to adherence problems to date has centered on the areas of structural adhesives and composites.^{11,12} Here, not only the analysis but also the measurements of crack tip stress intensity (K_I) can become quite complex even for crack motion along a flat interface between two materials because stresses acting on a crack are not symmetrical. Also, combined loading modes exist (e.g., mode I plus II), which greatly complicate the analysis. However, when the elastic properties E (Young's modulus) and ν (Poisson's ratio) of the two materials are comparable (in theory they must be identical¹³ but need only approach each other),¹⁴ then the mathematical solution is the same as for the crack in a single-phase body. This is the case for the analysis of adherence of many ceramic-to-ceramic and ceramic-to-metal systems. The result is that one can describe adherence in terms of K_{Ic} , rather than a complex combined K_I - K_{II} , and a much simpler description of crack propagation is obtained.

Experimentally, determination of the adherence of the system is simplified by use of the energy balance concept equating the change in the system's strain energy [the strain energy release rate (G_I)] with the total energy for crack propagation ($2\gamma_I$). Because the system acts as a homogeneous body, γ_I is related to K_I , i.e.,

$$K_I = \frac{\sigma c^{1/2}}{A} = (2\gamma_I E)^{1/2} \quad , \quad (4)$$

where σ is the tensile stress, acting on the joint, c is the flaw size, and A is a geometric factor; thus either γ_I or K_I can be determined

experimentally. Several experimental techniques have been evolved to determine the adherence not only of adhesives to metal but most recently of ceramics to metals or to other ceramics.¹⁵⁻¹⁷

EXPERIMENTAL PROCEDURE AND EQUIPMENT

SESSILE-DROP WETTABILITY

Our sessile-drop apparatus (Fig. 5) is essentially a horizontal induction-heated furnace unit, consisting of a fused silica tube 38 mm in diam and 300 mm long, in which a vacuum of 7 mPa (5×10^{-5} mm Hg) and temperatures to 1750°C can be obtained. An optical pyrometer is placed on one end of the furnace tube for direct viewing of the substrate, and an optical system to take photographs of the sessile drop at temperature is arranged at the other end. The tube contains dual-layer tantalum heat shields and a 15-mm-diam molybdenum susceptor. The specimen is contained

Y-190562

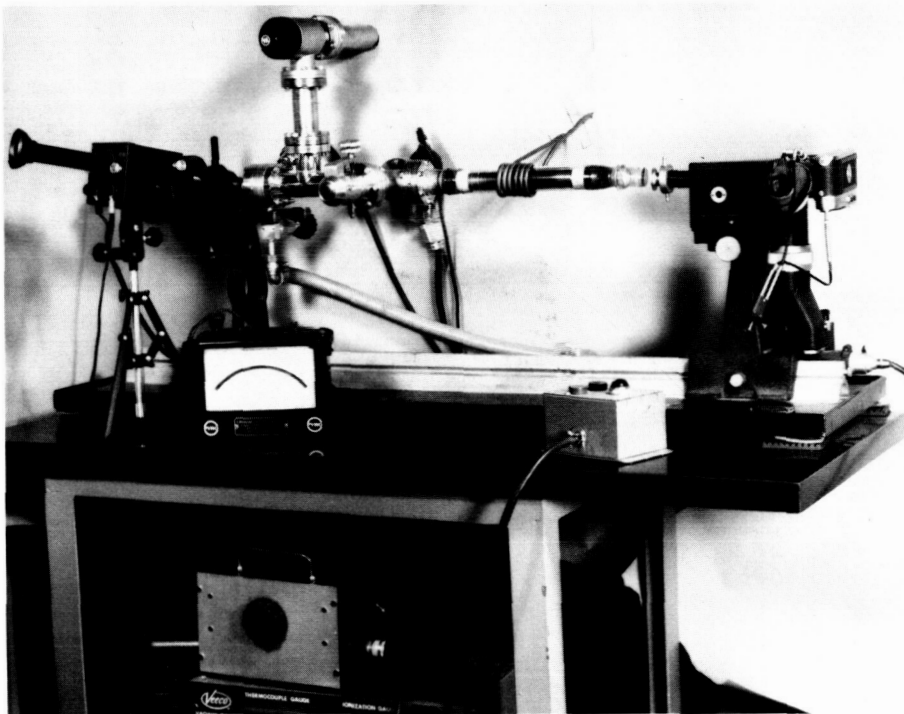


Fig. 5. Induction-heated, evacuated sessile-drop apparatus with temperature capability of 1750°C.

in a tantalum or ceramic boat. The advantage of induction heating is that it allows (if desired) rapid heating and cooling (because the thermal mass is small) so that the effect of relatively short times at temperature can be studied. From a practical standpoint, rapid heating and cooling is desirable so that three or four runs a day can be made. A potential disadvantage of this system is that if a gaseous environment (rather than vacuum) is desired, it is sometimes difficult to establish pressure conditions such that a glow discharge will not occur. Only vacuum was used in this work.

SESSILE-DROP SPECIMEN CHARACTERIZATION

After each run, a sessile-drop sample was removed from the tube, examined with a shadowgraph to measure the contact angle (for comparative purposes only), and then either sectioned for ceramographic examination or put into the apparatus shown schematically in Fig. 6 for determination of the apparent shear strength of the bond between the drop and the ceramic substrate. This device was developed by Sutton¹⁸ at General Electric Co., so its application is known as the Sutton push-off test. The test is a simple technique used to assess interfacial strength. Nicholas and coworkers at Harwell in England have studied this test and concluded that

ORNL-DWG 85-7799

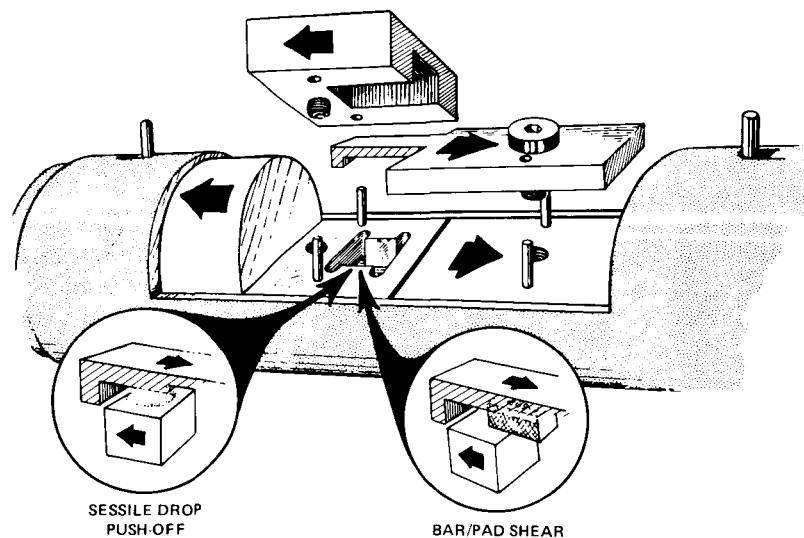


Fig. 6. Test fixture for determining shear strength of bond between a sessile drop of experimental brazing filler metal or a metal bar and a ceramic substrate pad.

for contact angles less than about 100° the test is a valid measure of shear strength.¹⁹ In all of our tests, the wetting angle has been considerably less than 100° .

This fixture is installed in a mechanical testing machine and the shear strength calculated from the load at failure divided by the interfacial area, which is determined prior to the test by using a toolmaker's microscope. Our shear tests for this work were done at room temperature.

Although we have in general been pleased with the push-off test as a rapid means of determining comparative bond strengths, our experiments have revealed a shortcoming. On samples in which the contact angle is low ($\ll 30^\circ$), the foot that pushes off the drop tends to ride up on the drop instead of pushing it off. In some cases a portion of the drop is eventually sheared off as can be seen in Fig. 7. In such a case the shear stress on the drop-substrate interface is calculated on the basis of the maximum load although failure has not occurred. For some of our best-wetting filler metals, we rely on three- or four-point bend tests rather than shear tests as a measure of bond strength.

Y-194144

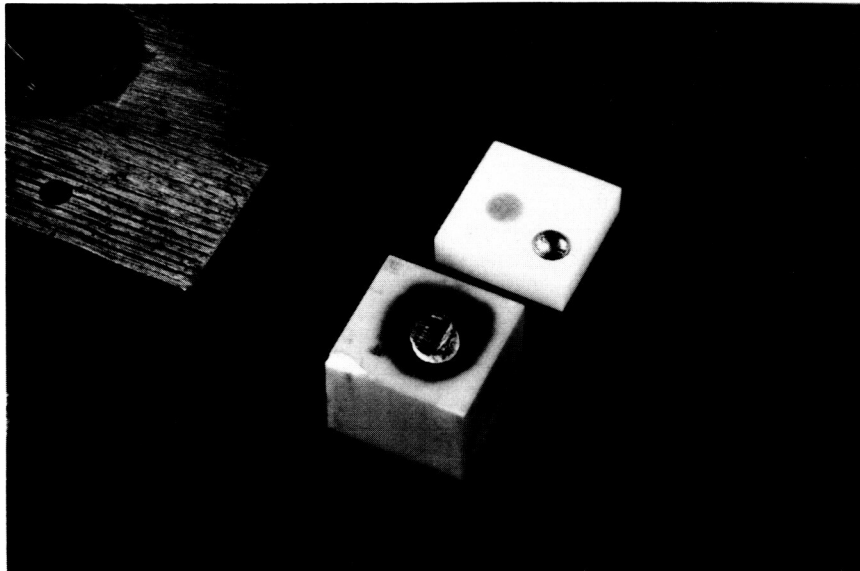


Fig. 7. Sessile-drop specimens after push-off test. In upper sample the drop has been removed by failure at the interface; in lower sample the drop itself has been sheared.

FLEXURAL STRENGTH MEASUREMENT OF BRAZED JOINTS

In addition to the shear tests on the sessile-drop specimens, flexural strength measurements have been conducted on ceramic-ceramic brazement samples joined with a number of our experimental brazing filler metals. Figure 8 shows the sequence of steps in fabricating the test specimens. Typically the specimens are tested in a side-bend configuration in a four-point bend fixture. Both room- and elevated-temperature tests (up to 600°C) have been conducted. In some cases brazing filler metal chunks were preplaced at the edge of the joint, but many times with that technique we did not obtain full penetration of the metal through the joint (~2 mm thick). We evaluated various joint gaps, which is typically how this problem is approached in brazing, but to no avail. Since these filler metals spread very readily over a flat surface, we concluded that metal-ceramic interactions at the front of the advancing capillary must be changing the local surface tension or interfacial energy and resulting in

ORNL-PHOTO 4957-84

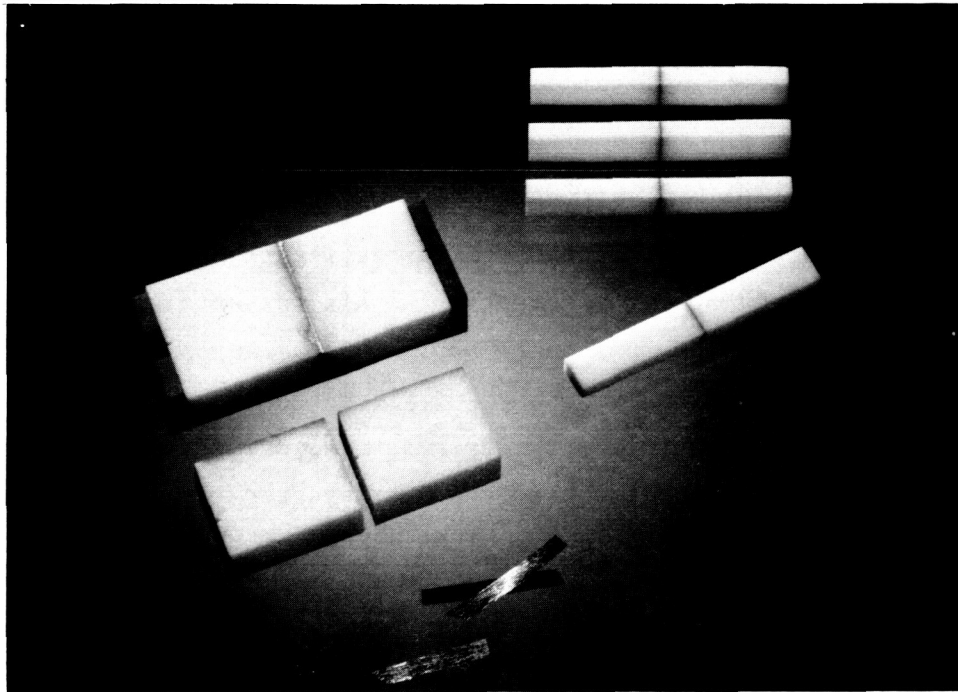


Fig. 8. Sequence of steps in fabricating flexural strength specimens containing a braze joint. In this example the filler metal was melt-spun foil.

reduced flow. Therefore, we had small quantities of experimental brazing filler metals in several alloy systems fabricated into narrow foils by melt-spinning to enable us to preplace the alloys in the joint. We have had good results with some of these foils and particularly with one from the Cu-Ag-Ti system.

CRITICAL FRACTURE TOUGHNESS, K_{Ic} , OF BRAZEMENTS

The specimen used is the same as one used to measure the fracture toughness of bulk structural ceramics — the applied moment double cantilever beam (DCB). A schematic diagram of the specimen prepared for measurement with arms attached is given in Fig. 9. The relationship used to determine K_{Ic} is simple:

$$K_{Ic} = \frac{M}{(tI)^{1/2}} \quad (5)$$

$$\text{where } M = P \cdot L \text{ and } I = \frac{bh^3}{12} \quad (6)$$

Thus, it can be seen that the fracture toughness of a brazement can be determined from the load at failure and some geometric factors if both arms of the DCB specimen are of the same material and size.

We evaluated both fine wires and thin foils between the specimen halves to control the final thickness of the braze joint and have settled on 0.038-mm tantalum foil because foil is easier to apply. Small pieces of the foil are held in place by cement.* We also experimented with various materials and designs of springs to apply loading across the joint during brazing and have found 0.25-mm-thick molybdenum or tungsten foil leaf springs to be satisfactory for the brazing temperatures used in most of our studies to date. Specimens in a SiC boat after brazing are shown in Fig. 10.

We also developed a standard procedure for preparing the samples for testing. After the samples are brazed they are ground to remove any exuded filler metal and to remove any mismatch of the surfaces. This operation is done by bonding the specimens to machining blocks with

*Microbraz Cement, Wall Colmonoy Corp., Detroit, Mich.

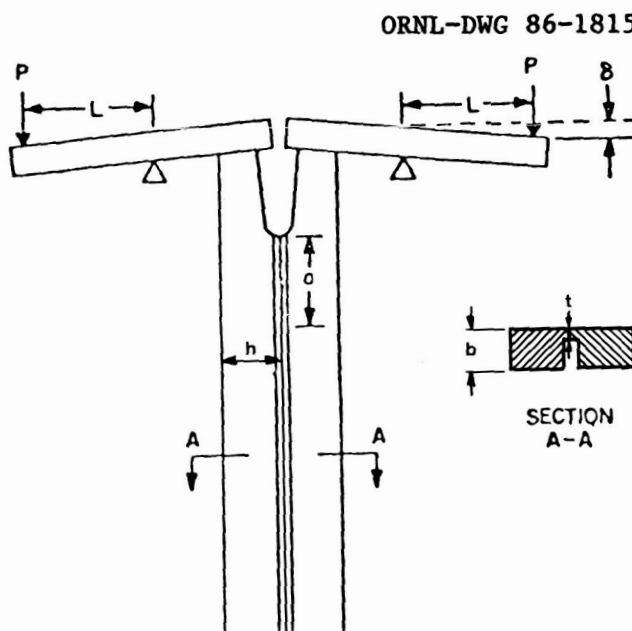


Fig. 9. Schematic diagram of double cantilever beam specimen after attachment of test arms. The precrack (shown to have a dimension " α ") is generated by forcing a wedge into the guide notch at the top of the specimen before the arms are attached.

ORNL-PHOTO 8023-85

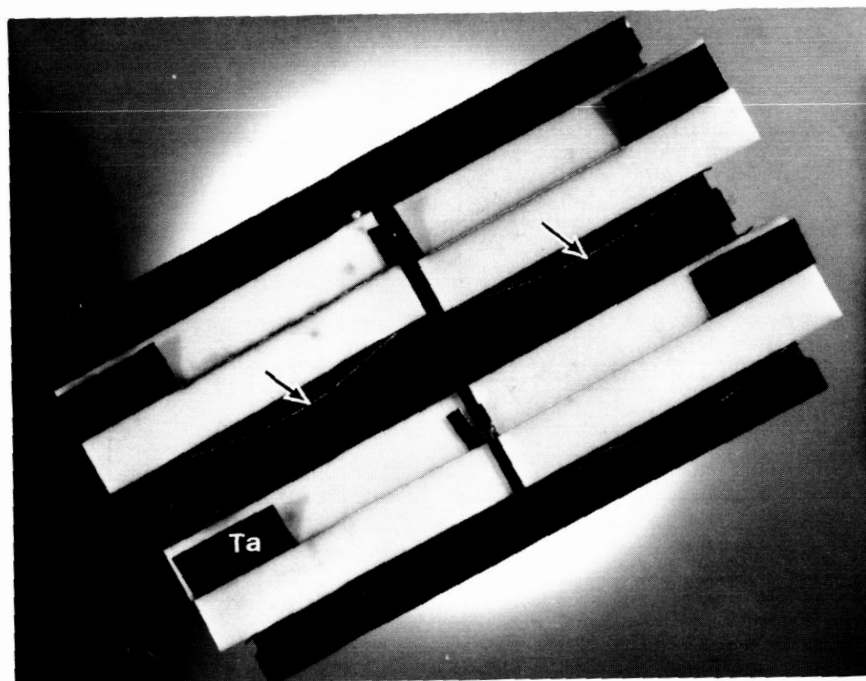


Fig. 10. Composite double cantilever beam specimens in a SiC boat after brazing. Loading across the joint is applied by molybdenum foil springs (arrows), and the brazing gap is limited to 0.038 mm by tantalum shims.

Crystalbond* 509 adhesive and then machine grinding with a 170-grit diamond abrasive wheel. After surface grinding, the specimens are grooved and notched to ensure that the crack will propagate through the region of the brazement. These operations are also done with diamond abrasive wheels (400 grit). The surface of the specimen opposite the groove is hand lapped with diamond paste (down to 3 μm). A final sharp precrack (flaw) is made in the braze joint by carefully forcing a hard TiB_2 wedge into the large notch of the specimen. This operation is conducted under a low-power microscope so that the flaw (crack) can be observed as it forms.

As is the case for bulk ceramic specimens, the loading arms are attached with epoxy cement taking care that the fulcrum lengths " L " are equal and that the specimen is perpendicular to the arms in two planes. After the epoxy is cured, the specimens are loaded in a mechanical test apparatus (Fig. 11). The load at failure and specimen dimensions (b , h , and t) are recorded.

SHEAR STRENGTH OF CERAMIC-METAL BRAZEMENTS.

In order to determine the shear strength of ceramic-metal brazements we developed a "bar/pad" specimen that is tested in the same fixture as the sessile-drop specimens. In this test (shown schematically in Fig. 6) a metal bar having dimensions of $3.18 \times 3.18 \times 9.52$ mm is brazed to a 9.52×9.52 mm ceramic pad whose thickness depends on the material thickness. The bar overlaps the pad by 6.35 mm. A typical specimen is shown in Fig. 12. The specimens are held together for brazing by fine molybdenum wires that also serve to apply a load across the joint because of the difference in coefficients of thermal expansion of the components and wires. The shear strength is calculated on the basis of the load at failure and the overlap area. These brazing filler metals produce very small fillets that are ignored in the calculation.

*Aremco Products, Inc., Ossining, N.Y.

CYN-5387

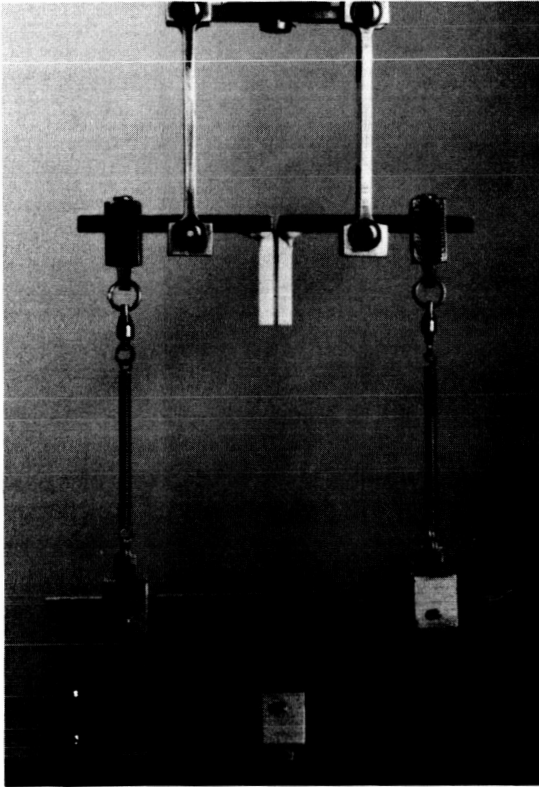
ORIGINAL PAGE IS
OF POOR QUALITY

Fig. 11. Apparatus for testing composite double cantilever beam specimens in mechanical test machine.

ORNL-PHOTO 6292-84

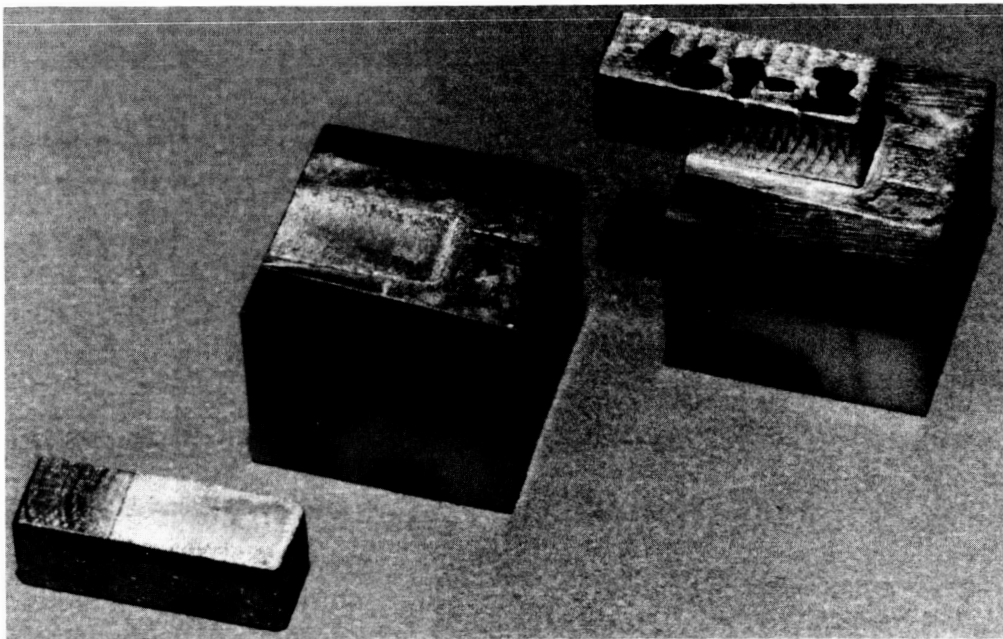


Fig. 12. Bar/pad shear test specimens. The metal bars have dimensions of $3.18 \times 3.18 \times 9.52$ mm and overlap the pads by 6.35 mm. The partially stabilized zirconia pads measure $9.52 \times 9.52 \times 7.62$ mm.

MATERIALS

STRUCTURAL CERAMICS

Some of the characteristics of the ceramic materials included in this study are given in Table 2. (A few small pieces of NGK Z191 tetragonal zirconia polycrystalline ceramic were used in wettability studies but were not otherwise characterized.) All of the ceramics were fabricated by pressureless sintering except for our experimental SiC-whisker-reinforced Al_2O_3 composite, which was hot pressed. These specific materials were chosen because they are prime candidates, or potential alternates, for insulating components in the uncooled diesel engine.

Table 2. Characteristics of ceramic materials brazed in this program

Material designation	Flexural strength (MPa)	Average ^a surface roughness (μm)
Coors AD-99 alumina	230 ^b	0.74
Coors AD-998 alumina	207 ^c	2.65
Degussit AL-23 alumina	156	4.46
Nilsen PSZ (82-94159N)	616 ^b	0.94
Nilsen PSZ (83-064MS)	574 ^b	0.94
Al_2O_3 -SiC ^d	650	

^aDetermined by profilometer.

^bRoom temperature, four-point bend (6.35- and 19.0-mm spans), crosshead speed of 0.085 mm/s.

^cSame except 6.35- and 12.7-mm spans.

^dSiC-whisker-reinforced alumina under development at ORNL.

Partially stabilized zirconia has low thermal conductivity and high toughness for a ceramic and relatively high thermal expansion and is thus the prime candidate for insulating the combustion chamber of the uncooled diesel engine. However, the microstructure of the MgO-stabilized PSZs presently available is not stable at or above about 800°C because there is

a loss in the amount of the tetragonal phase, which provides high toughness, and because the cubic phase transforms to monoclinic phase after prolonged time at temperature. Even for short times those PSZs are less tough at elevated temperatures because of the reduced tendency for the tetragonal to monoclinic phase transformation.²⁰

A fine-grained yttria-stabilized tetragonal zirconia (referred to as tetragonal zirconia polycrystals or TZP) was obtained from Cummins Engine Company, Inc., for a comparative wettability study using our experimental brazing filler metals. This material, designated NGK Z-191, is being considered as an alternate material for MgO-stabilized PSZ in the uncooled diesel engine. The Y_2O_3 -stabilized TZP ceramics are presently thought to be more resistant to the overaging phenomena observed in the MgO-stabilized materials in which thermally induced phase changes lead to a loss of strength and toughness with time at temperature.

Several high-alumina ceramics were selected in order to assess the effect of purity levels and manufacturer (who might, for example, use different sintering aids) on wetting and bonding in the experimental brazements. The Al_2O_3 -SiC composite was included because it has excellent toughness and strength at both room and elevated temperatures. Although this composite as presently formulated has significantly greater thermal conductivity than PSZ [~ 11 W/(m \cdot K) vs 2.4 W/(m \cdot K) at 800°C], we and others are investigating several techniques to reduce its conductivity.

The surface of each of the ceramic materials that were brazed in the wettability tests is shown in Figs. 13-18. In general for the AD-998 and AL-23 alumina materials, the brazed surface was in the as-fired condition (other than a thermal treatment of 15 min at 1000°C to clean the surface); for the other materials, the surface was ground.

STRUCTURAL METALS

The nodular cast iron material used in the ceramic metal brazements in this study was provided by Cummins Engine Company, Inc., from a portion of a piston made by Izumi in Japan. The microstructure of the cast iron as received was primarily pearlite with some ferrite plus nodules of

M-20152

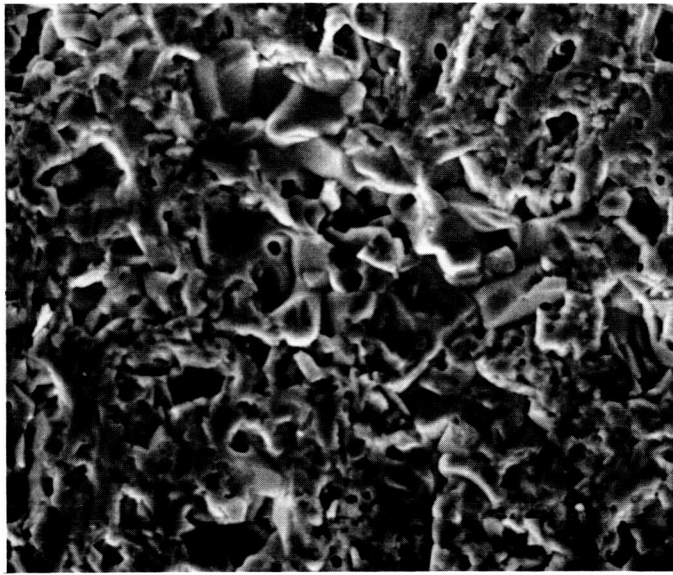
10 μm

Fig. 13. Scanning electron micrograph of AD-99 alumina substrate used in sessile-drop wettability study.

M-20206

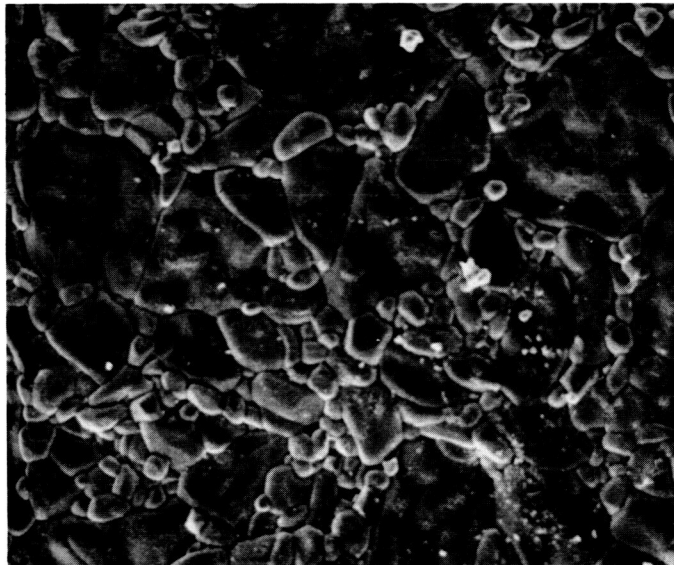
10 μm

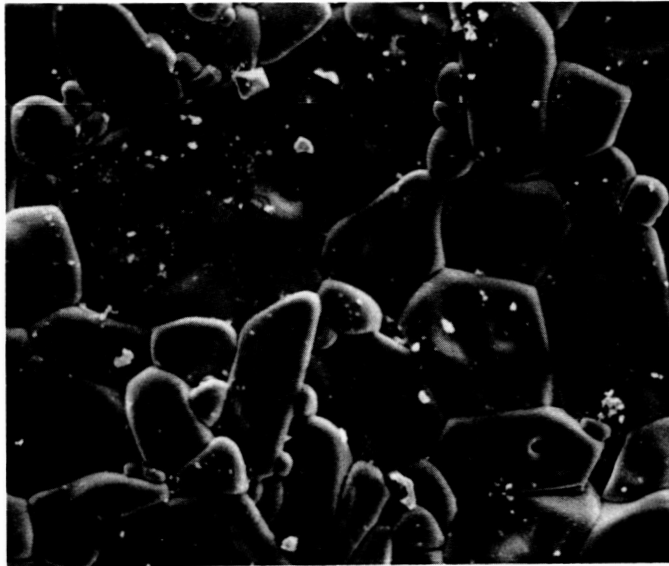
Fig. 14. Scanning electron micrograph of surface of AD-998 alumina.



10 μ m

Fig. 15. Scanning electron micrograph of Degussit AL-23 alumina substrate.

ORNL-PHOTO 7588-84



10 μ m

Fig. 16. Scanning electron micrograph of Nilsen TS grade PSZ (82-94159N) substrate.

ORNL-PHOTO 7583-84

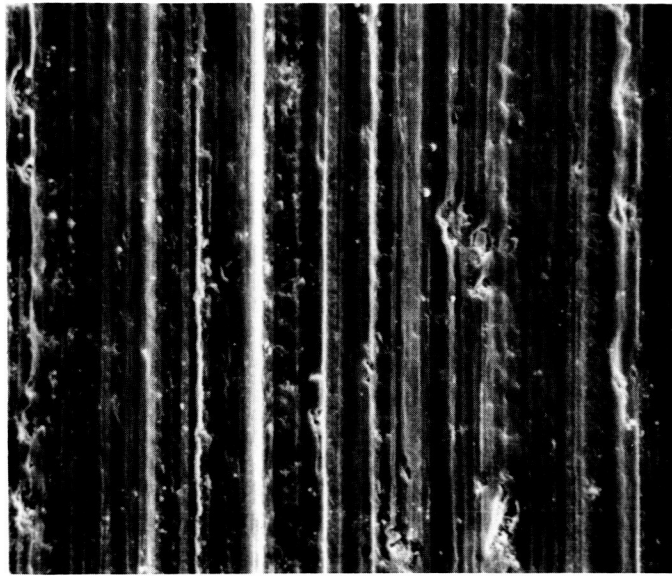
10 μm

Fig. 17. Scanning electron micrograph of surface of Nilsen MS grade PSZ (83-064 MS).

ORNL-PHOTO 7589-84

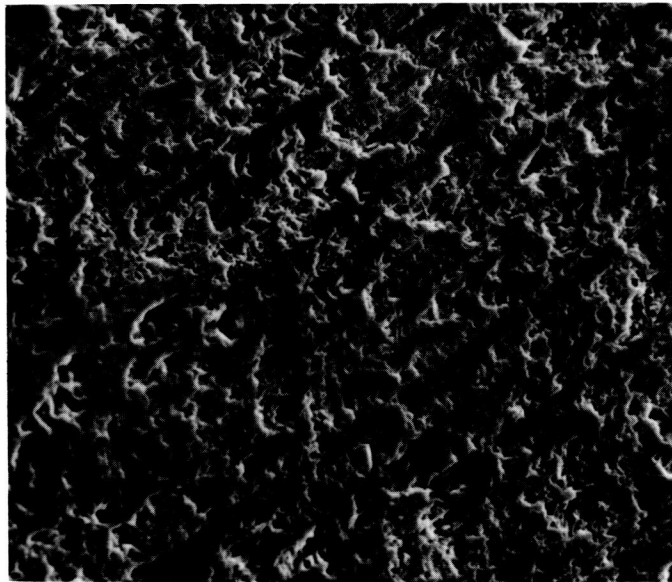
10 μm

Fig. 18. Scanning electron micrograph of surface of SiC-whisker-reinforced alumina composite made by hot pressing at ORNL.

graphite. A microstructure high in the pearlitic phase is thought to be desirable in the pistons of advanced heavy-duty diesels because such a material is reported to have the desirable high-cycle fatigue strength. The lower critical temperature for this iron is about 725°C, which means that, to attain a final pearlitic piston, the brazing temperature for a ceramic attachment would have to be about 725 to 750°C (depending on the kinetics of the pearlite → austenite transformation) or else above that temperature with a subsequent rate of cooling such that pearlite and not bainite or martensite is formed. The coefficient of thermal expansion for this iron is about $14 \times 10^{-6}/^{\circ}\text{C}$, lower than that of many common structural metals but probably not similar enough to that of PSZ and alumina to avoid problems associated with differential shrinkage strains.

Titanium and type 446 stainless steel were also included in this study, because they could be used as ductile transition materials to accommodate the mismatch in coefficients of thermal expansion of the cast iron and structural ceramics.

EXPERIMENTAL FILLER METALS

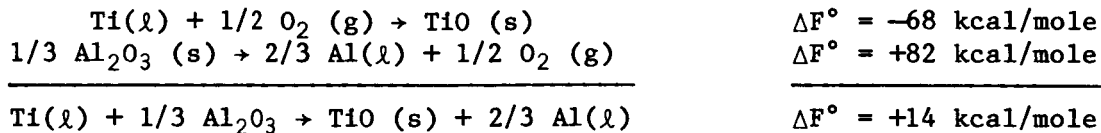
Several criteria must be met for a brazing filler metal to meet the joining requirements for a given application:

1. The filler metal must wet the ceramic and/or metals of interest.
2. Relatively strong bonds must be formed that will survive not only cool-down from brazing temperature but also service conditions.
3. The filler metal and/or brazing process must not degrade the base material(s).

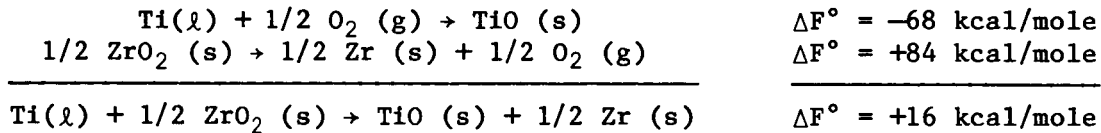
With these criteria in mind, we formulated potential filler metals that would wet and adhere to alumina, PSZ ceramics, and nodular cast iron at brazing temperatures that would cause minimal deterioration of the materials. The intended service environment was assumed to be air at 400°C or less.

Experimental studies on brazing of ceramics have shown that the affinity of the filler metal or elements in the filler metal for oxygen (in the case of oxide ceramics) or for carbon (in carbides) plays a crucial role in determining the strength of the brazed interface. Although some treatments of the subject have tried to explain this behavior simply on

the basis of free energies of formation of stable oxides of metals in the filler metal (and therefore reduction of the ceramic at the interface to a metal), this explanation is not sufficient. On the basis of oxidation-reduction reactions alone, titanium should not react with alumina or zirconia ceramics even at very high temperatures.²¹ For example the following reactions are applicable at 1800°C.



and,



Thus, on the basis of these reactions, Al_2O_3 and ZrO_2 would be more stable because of their lower free energies of formation. However, titanium has in many studies been found to react with oxide ceramics, and all filler metals known to the authors for joining of oxide ceramics have contained titanium, either singularly or in combination with zirconium or other strong oxide-forming elements. We think this apparent anomaly can be explained on the basis of the free energies of solution of oxygen in the titanium and to a lesser degree on the solubility of aluminum (in the case of alumina) in titanium. Oxygen is soluble in titanium up to 34 at. % (independent of temperature),²² and aluminum is soluble up to 15 at. % (at 1000°C). Consequently, reactions may proceed with the reaction products soluble to a considerable extent in the molten filler metal. However, the activity coefficients for these solutions are not known at this time, so we were required to formulate the experimental brazing filler metals on the basis of empirical results.

We used as the basic compositions three binary alloy systems (Ag-Cu, Cu-Au, and Au-Ni) and one ternary system (Cu-Au-Ni). These alloys are widely used by the brazing industry, have simple microstructures, and have relatively low brazing temperatures. Titanium was chosen as the reactive element in each composition.

The filler metals were produced by one of three techniques: (1) arc melting of a button (1-2 g) on a water-cooled copper hearth, with the drop flattened after the sixth melt cycle; (2) arc melting of a button (~125 g) that is drop cast into an 11-mm-diam cylindrical copper mold; or (3) induction melting of a sample (~5 g) in a helium atmosphere and then rapidly solidifying by casting onto a rotating copper wheel.

The apparatus used for melting the small buttons of material is shown in Fig. 19. The procedure used is to evacuate the chamber to a pressure less than 3 mPa (2×10^{-5} mm Hg), backfill to slightly greater than atmospheric pressure with high-purity argon, melt a zirconium getter button, and then melt the charge six times, turning it over after each melt. Prior to the final melting the ingot is moved to a concave copper pad in which it is formed by a convex tungsten ram prior to solidification. The advantages of this equipment are that it minimizes the amount of material needed for a cursory evaluation of a given composition and, because of the flattening operation, produces a sample that can be cut into small pieces by using pliers rather than having to resort to rolling into foil or using abrasive cutting wheels. A disadvantage of the small melt is that insufficient material is produced for chemical analysis so that we have to rely on careful weighing before and after melting as an indication of potential composition changes from evaporation or spatter, or contamination by reaction with the electrode.

As mentioned previously we have also had two compositions (MWF-2, Cu-26 Ag-29 Ti, and MWF-7, Cu-20 Au-18 Ti, at. %) made into foil by melt spinning. This work is in a very preliminary stage, but the results have been encouraging.

EXPERIMENTAL RESULTS

At this stage of the program we have been characterizing the wetting and bonding behavior of a broad range of metallic filler metals on a spectrum of structural oxide ceramic substrates. We conclude that at least two of the alloy systems (Cu-Ag-Ti and Cu-Au-Ti) show promise of providing a useful brazing filler metal for application in the uncooled diesel. Each is discussed below.

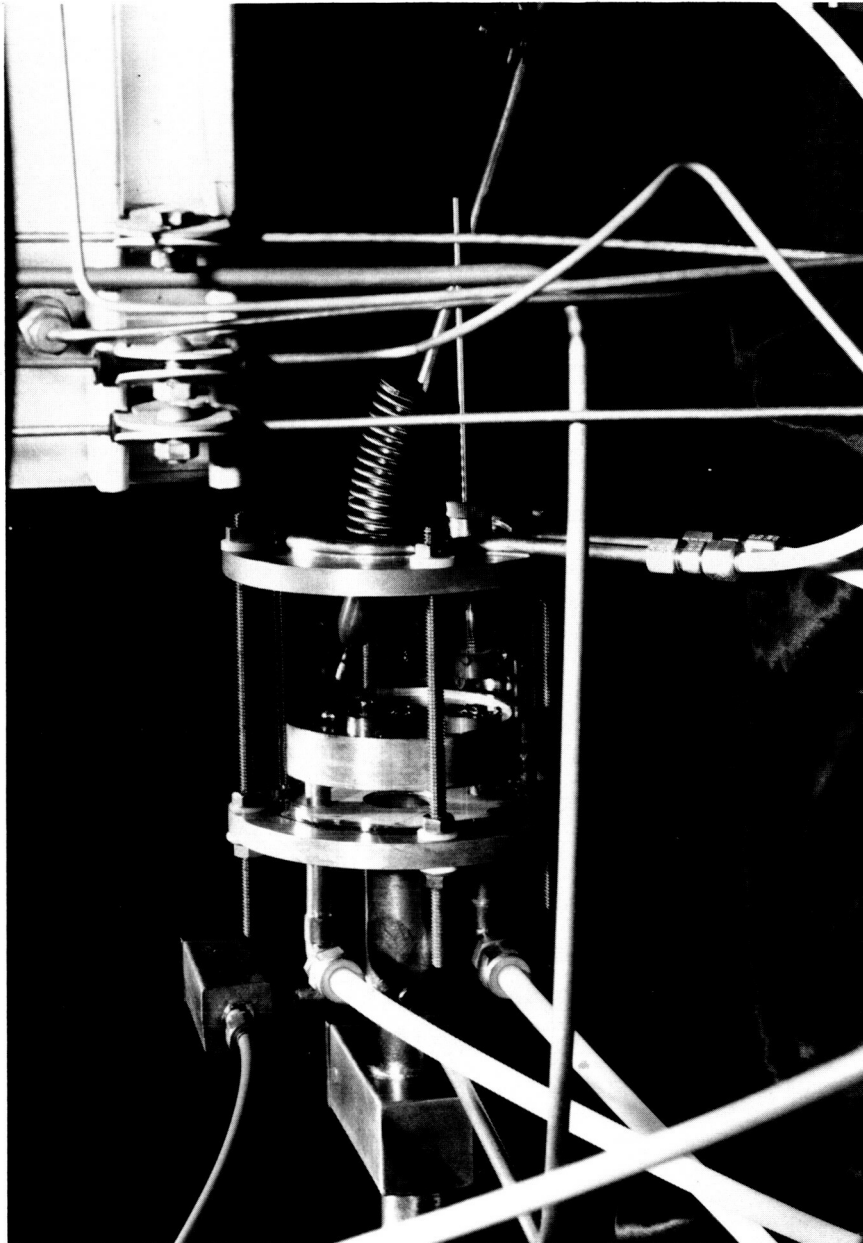


Fig. 19. Arc melter used to fabricate small quantities of experimental brazing filler metals.

SILVER AND COPPER BASED SYSTEM

This system is based on the silver-copper eutectic that occurs at 40 at. % Cu and 780°C. A wide range of commercial brazing filler metals

are based on this system, and one, with a composition of Ag-37 Cu-8 Ti, at. %, was known to wet and bond to some ceramic materials. A small addition of nickel is sometimes added to the basic Ag-40 Cu eutectic to improve wetting and corrosion resistance, so our study also included three Ag-Cu-Ni-Ti quaternary compositions as shown in Table 3.

Table 3. Experimental filler metals in the Ag-Cu system

Alloy designation	Composition (at. %)	Brazing range ^a (°C)
MWF-1	Cu-27 Ag-26 Ti	900-950
-2	Cu-26 Ag-29 Ti	920-1000
-42	Ag-38 Cu-1 Ni-4 Ti	950-1050
-43	Ag-37 Cu-0.75 Ni-7.25 Ti	850-950
-44	Ag-35 Cu-0.7 Ni-10.3 Ti	950-1050

^aBrazing temperature depends to some degree on substrate material and on the extent of flow desired.

The flexural strength data for brazements made with filler metals in the Cu-Ag-Ti system are given in Table 4 and shown graphically in Fig. 20. Note that there are no shear strength data (another important engineering property) for any of the compositions in this series. All of these filler metals wet all of the alumina and zirconia ceramics so well ($\theta < 15^\circ$ on all substrates) that we were unable to obtain a valid shear strength by using the push-off test. In those cases where such a test was attempted, the foot of the test fixture simply rode up on the drop, occasionally shearing away part of the drop. We selected a representative of this group (MWF-2, Cu-26 Ag-29 Ti, at. %) with which to conduct the majority of the mechanical property tests because this filler metal seemed to be the most consistent in wettability behavior.

The data show that this filler metal produces strong bonds in joining the two aluminas with strengths approximating those of the bulk ceramics. In fact, in some samples, failure occurred in the ceramic itself rather than in the joint area. The strength of the brazements in the PSZ material was only about half the strength of the bulk ceramic, but these values are

Table 4. Summary of flexural strength data for experimental brazing filler metal MWF-2, Cu-26 Ag-29 Ti, at. %

Specimen number	Temperature (°C)		Number of specimens	Mean strength (MPa)	Standard deviation	Location of failure
	Brazing ^a	Test ^b				
AD-998 alumina						
414	980	25	4	222 ^c	33	Ceramic
394	1010	400	4	215 ^d	37	Mixed ^e
395	1010	600	4	213 ^d	24	Joint
AL-23 alumina						
356	1090	25	4	91 ^c	49	Ceramic
392	1010	200	2	145 ^c	1	Mixed
392	1010	400	2	110 ^c	28	Mixed
415	980	400	4	165 ^d	41	Mixed
PSZ (83-064 MS, MgO stabilized)						
348	1040	25	4	350 ^c	41	Joint
353	1100	25	4	294 ^c	67	Joint
362	1010	25	4	339 ^c	53	Joint
391	1010	200	2	159 ^c	26	Joint
391	1010	400	2	132 ^c	70	Joint

^aAll brazing in vacuum of less than 7 mPa ($<5 \times 10^{-5}$ mm Hg) at start of cycle, about 27 mPa ($\sim 2 \times 10^{-4}$ mm Hg) at temperature.

^bAll tests in air, 30 min at temperature prior to testing.

^cCrosshead speed of 0.085 mm/s, four-point bend, 6.35- and 25.4-mm spans.

^dLoad rate of 22.7 kg/s, four-point bend, 6.35- and 19.0-mm spans.

^eSome samples failed in braze joint, others in ceramic.

still very respectable because the PSZ has very high flexure strength, greater than 600 MPa. The brazements in the aluminas also appear to maintain their strengths better at elevated temperature than do those in PSZ, but with the rather limited amount of test data it is too early to draw any firm conclusions or to search for possible mechanisms that might explain such behavior.

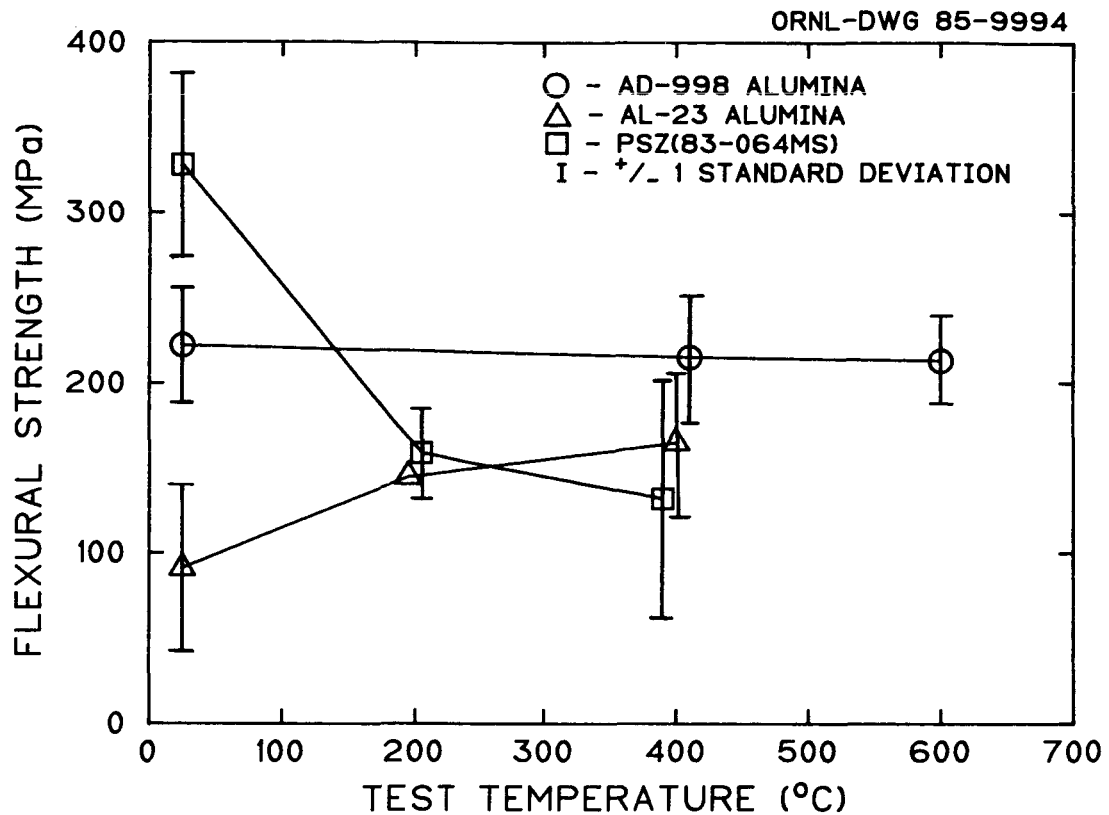


Fig. 20. Flexural tests (in air) of structural ceramics brazed in vacuum with filler metal MWF-2, Cu-26 Ag-29 Ti, at. %.

COPPER AND GOLD BASED SYSTEMS

Three series of filler metals with gold as a major constituent were evaluated with the following commercial alloys as the base compositions: (1) Cu-15 Au-4 Ni (at. %), 1030°C liquidus, 1000°C solidus; (2) Au-43 Cu, 970°C liquidus, 955°C solidus; and (3) Au-42 Ni, 950°C solidus and liquidus. The gold based filler metals are widely used, are generally more corrosion resistant than the silver based alloys, but also are more expensive and have higher brazing temperatures. These series include the compositions listed in Table 5.

The shear and flexural strength data for ceramic-ceramic brazements made with these filler metals are given in Tables 6 to 9. These data show that the Cu-Au-Ni-Ti system shows little promise, but that the Cu-Au-Ti system has good potential. Here again, as with the Cu-Ag-Ti filler metals, flexural strengths of the alumina brazements are very respectable even up

Table 5. Experimental brazing filler metals with copper and gold as major elements

Alloy designation	Composition (at. %)	Brazing range ^a (°C)
MWF-4	Cu-14 Au-4 Ni-6.5 Ti	1090-1190
-5	Cu-13 Au-3.5 Ni-14 Ti	1050-1150
-6	Cu-22 Au-10 Ti	1350-1450
-7	Cu-20 Au-18 Ti	1050-1150
-8	Cu-18 Au-26 Ti	1050-1150
-9	Au-36 Ni-11 Ti	1050-1200
-10	Au-30 Ni-21 Ti	1150-1250

^aBrazing temperature depends to some degree on substrate material and on the extent of flow desired.

Table 6. Wetting and bonding behavior of experimental filler metals in Cu-Au-Ni-Ti series on alumina ceramics

Specimen number	Substrate	Brazing ^a temperature (°C)	Wetting angle ^b θ (°)	Shear strength (MPa)
MWF-4 (Cu-14 Au-4 Ni-6.5 Ti, at. %)				
462	AL-23	1300	90	DNA ^c
463	AD-998	1350	90	DNA
MWF-5 (Cu-13 Au-3.5 Ni-14 Ti)				
301	AD-998	1150	60/70 ^d	14.7
304	AL-23	1150	30/40	>22
315	AL-23	1150	30	<i>e</i>
464	AL-23	1340	180	DNA
465	AD-998	1260	10/30	21

^aBrazed in vacuum of less than 7 mPa ($<5 \times 10^{-5}$ mm Hg) at start of cycle, about 27 mPa ($\sim 2 \times 10^{-4}$ mm Hg) at temperature.

^bMeasured at room temperature.

^cDrop had no indication of adherence.

^dIrregular drop, angles measured 90° apart.

^eSeparated at the interface on cooling to room temperature.

Table 7. Wetting and room-temperature shear strength of bonds between filler metals in Cu-Au-Ti series and alumina substrates

Specimen number	Substrate	Brazing temperature (°C)	Wetting angle θ (°)	Shear strength (MPa)	Remarks
MWF-6 (Cu-22 Au-10 Ti, at. %)					
302	AD-998	1150			<i>a</i>
307	AL-23	1550	90		<i>b</i>
316	AL-23	1440	90		<i>b</i>
447	AD-998	1500	90		<i>b</i>
448	AD-998	1510	90		<i>b</i>
MWF-7 (Cu-20 Au-18 Ti, at. %)					
222	AD-99	1230	20	>70	
308	AL-23	1220	30	123	
317	AL-23	1120	60/70 ^c	90	
318	AL-23	1100	70	32	
318	AL-23	1100	70	28	
332	AD-998	1140	50	106	
336	AD-998	1185	25/30	74	
366	SC-79	1090	40/50		<i>d</i>
374	SC-79	1130	40	>72	
449	AD-998	1240	40	28	
450	AD-998	1240	40	30	
451	AD-998	1140	40	27	
MWF-8 (Cu-18 Au-26 Ti, at. %)					
309	AL-23	1250	10		<i>d</i>
310	AL-23	1160	40	115	
319	AL-23	1150	50	72	
319	AL-23	1150	50	60	
452	AD-998	1160	40	55	
453	AL-23	1160	40	118	
460	AL-23	1175	40	38	
461	AD-998	1175	40	76	
466	AD-998	1160	30	82	

^aDid not melt at that temperature.

^bDid not adhere.

^cIrregular drop, angles measured 90° apart.

^dInterface separation.

Table 8. Flexural strength of alumina and zirconia ceramics
 brazed to themselves with filler metal MWF-7
 (Cu-20 Au-18 Ti, at. %)

Specimen number	Temperature (°C)		Number of specimens	Mean strength (MPa)	Standard deviation	Location of failure
	Brazing	Test				
AD-998 alumina						
467	1070	25	4	257	23	Ceramic
412	1070	400	4	218	44	Joint
AL-23 alumina						
357	1130	25	3	93	51	Mixed
393	1200	400	4	106	24	Joint
416	1040	600	3	95	7	Joint
PSZ (83-064MS)						
367	1150	25	4	258	66	Joint

Table 9. Wetting and bonding behavior of sessile drops
 in Au-Ni-Ti series on alumina substrates

Specimen number	Substrate	Brazing ^a temperature (°C)	Wetting angle ^b θ (°)	Shear strength (MPa)	Remarks
MWF-9 (Au-36 Ni-11 Ti, at. %)					
311	AL-23	1210	80	37	<i>c</i>
MWF-10 (Au-30 Ni-21 Ti, at. %)					
312	AL-23	1320	40	33	

^aAll brazes conducted with system evacuated to less than 7 mPa ($<5 \times 10^{-5}$ mm Hg) at start of cycle, about 27 mPa ($\sim 2 \times 10^{-4}$ mm Hg) at brazing temperature.

^bMeasured at room temperature.

^cTore out crater in alumina during shear test.

to 600°C. For example at 400°C the flexural strength of AD-998 alumina brazed with Cu-20 Au-18 Ti was 218 MPa and of AL-23 alumina at 600°C was 95 MPa. Note that the wetting angles for these filler metals are greater than those for the Cu-Ag-Ti materials, but still low enough for practical use in brazing.

FRACTURE TOUGHNESS OF THE BRAZEMENTS

Only a limited number of fracture toughness tests have been conducted on samples brazed with filler metals from the silver- or gold-base systems because of problems with flow of the filler metal through the joint when it had been preplaced on the surface. The fabrication of foil by melt spinning has alleviated this problem to some extent, although we still have not achieved a high-quality foil of the Cu-Au-Ti composition. However, the results to date (Table 10) have been encouraging in that the critical fracture toughness, K_{Ic} , of the brazed samples has been at least as great as that of the bulk ceramic, and so far we have done nothing to optimize, through compositional variations or thermal cycle, the toughness of these brazements. We will conduct more of these important tests on both ceramic-ceramic and ceramic-metal specimens in our ECUT-funded work. We also plan to develop a specimen suitable for measuring the fracture toughness of brazements at elevated temperatures, as well as a Mode II (shear) specimen.

Table 10. Fracture toughness of brazements in PSZ ceramic^a joined with experimental brazing filler metal of composition Cu-27 Ag-26 Ti, at. %

Specimen number	Brazing temperature (°C)	Time at temperature (min)	Fracture toughness (MPa·m ^{1/2})
103	1000-1010	5	7.2
104	1010	5	6.6
105	1040	4	5.9
107	1010	20	6.1

^aNilsen 82-94159N having fracture toughness, as determined by double cantilever beam specimen, of 6.0 MPa·m^{1/2}.

SHEAR STRENGTH OF THE CERAMIC-METAL JOINTS

Partially stabilized zirconia ceramic-to-metal specimens were brazed in a bar/pad geometry (Fig. 12) with preplaced melt-spun foil of composition Cu-26 Ag-29 Ti, at. %. The PSZ was Nilsen MgO stabilized (83-064 MS), and the metal bars were either nodular cast iron (Izumi material supplied by Cummins Engine Co.), type 446 stainless steel, or commercially pure titanium. Most of these samples were brazed in vacuum at 1000°C, a temperature that had resulted in strong PSZ-to-PSZ brazements (339 MPa flexural strength) in our earlier work.

The room-temperature shear test results for this series of brazements are given in Table 11. The samples were tested in the same apparatus shown previously that was used to shear the sessile drops for bond strength measurements. We are very pleased by the high strength values for some of the PSZ/NCI and PSZ/446 brazements. We are presently trying to determine what is responsible for the low values observed, as all variables were maintained as constant as possible. We also are studying lower-temperature braze cycles to determine if they improve the disappointing results for the PSZ/titanium brazements. In these samples there was considerable dissolution of the titanium bars, indicating that the temperature was too high.

DISCUSSION OF RESULTS

During the course of this investigation several observations were made that deserve amplification: (1) the variability in bond strength data, (2) the effect of active-metal-containing filler metals on PSZ, (3) the difference in wetting behavior of our filler metals on MgO-stabilized PSZ versus Y_2O_3 -stabilized TZP, and (4) the effect of a 1000°C brazing cycle on nodular cast iron. These topics are discussed below.

VARIABILITY IN BOND STRENGTH DATA

An area of continuing concern throughout this work has been the wide range in shear- or flexural-strength values observed for samples that were

Table 11. Room-temperature shear strength of metal-ceramic bar/pad specimens brazed in vacuum at 1000°C with Cu-26 Ag-29 Ti, at. %

Specimen number	Materials		Shear strength (MPa)	Remarks
	Bar	Pad		
470-1	NCI	PSZ ^a	205	<i>b</i>
-2			19	
-3			20	
471-1	NCI	PSZ	19	
-2			30	
-3			183	
479-1	NCI	PSZ	122	10 min at temperature
-2			18	
480-1	NCI	PSZ	30	
-2			20	
481-1	NCI	PSZ	25	Brazed at 980°C
-2			36	
469-1	446	PSZ	52	
-2			205	
-3			>218 ^c	
472-1	446	AD-998	17	
-2			63	
-3			43	
468-1	Ti	PSZ	21	
-2			22	
-3			32	

^aNilsen 83-064MS.

^bAll samples with same batch number (e.g., 470) brazed at one time in vacuum of about 7 mPa ($\sim 5 \times 10^{-5}$ mm Hg). Five minutes at temperature unless otherwise indicated.

^cTest reached capacity of load cell.

supposedly of the same materials and processed in the same manner. Some of the variability could be attributable to processing variables such as slight differences in brazing temperature (e.g., specimens 317 and 318 of Table 7 with a 20°C difference in brazing temperature but a 3× difference in shear strength). In other cases there is an unexplained large difference in bond strength for samples supposedly brazed under identical conditions (e.g., samples 332 and 451 of Table 7 with shear strengths ranging from 27 to 106 MPa). Although such variations in shear strength data have also been observed by other investigations both in brazing²³ and in thick films,²⁴ it is disturbing nonetheless. In our review of the literature we have found no work that has attempted to directly resolve this critical issue that affects the potential reproducibility and reliability of brazements. Of course this behavior could be the result of normal variations in flaw or defect sizes in the ceramics influencing braze joints with modest toughness.

We have also observed significant differences between samples that were brazed at the same time. These brazes were conducted in the sessile-drop apparatus, which uses induction heating and a molybdenum tubular susceptor. The samples were arranged axially along the susceptor and immediately adjacent to each other. The temperature was monitored by optically sighting on one ceramic substrate, but the second sample was obscured from view. Although it seems unlikely that there was sufficient temperature difference between specimens to cause a large difference in shear strengths, we decided to stop the practice of brazing two samples at a time, to eliminate this practice as a possible source of the variability.

Another possible reason for sample-to-sample bond strength variations could be differences in surface roughness. The effect of surface roughness on wetting and/or bonding has been observed by others. For example, Rhee²⁵ reported that aluminum sessile drops on TiB₂ or TiN went from non-wetting ($\theta > 90^\circ$) to wetting ($\theta < 90^\circ$) as the surface finish was changed from rough ("as hot pressed") to smooth ("mirror finish"). We at one time postulated that the surface finish on one side of our ceramic substrate blanks might be different from that of the other so that the sessile-drop shear strength would be high or low depending on whether a smooth or rough

surface was being brazed. However, careful measurements with a profilometer showed that in all cases the surface finishes of both sides of the material were nearly the same.

Becher and Murday²⁴ attributed observed differences in thick-film adherence fracture energies to surface layers of glasses that were present on alumina substrates either after processing or after subsequent firing during thick-film application. For example, they reported surface layers consisting of up to 25 wt % SiO₂ in as-received 99+ wt % alumina substrate in which the bulk SiO₂ content was less than 1%. They observed an approximately two-fold change in fracture energy for two aluminas depending on firing temperature. Therefore, we conducted a brief study on several of our alumina substrates looking for surface layers that might explain our observed variability in sessile-drop shear strength. The substrate materials and their history prior to examination are listed below:

1. Coors AD-99 alumina - as received;
2. Coors AD-998 alumina - fired in air for 15 min at 1000°C;
3. AD-998 alumina - same as (2) followed by leaching 2 h in 20 vol % HF;
4. Degussit AL-23 alumina - as received;
5. AL-23 alumina - fired in air 15 min at 1000°C; and
6. A series of alumina substrates all of which had been in contact at about 1550°C with a drop of MWF-21 (Ni-14 Al-10 Ti-0.2 B, at. %), a filler metal being studied in the ECUT program.

We employed an ISI-SS40 scanning electron microscope with analytical capabilities including a Tracor Northern TN2000 energy dispersive X-ray analysis (EDAX) system. This equipment is sensitive to elemental levels of about 1/2 wt %. All samples were coated with carbon prior to examination.

The results give an indication of a potential cause for the observed variability. In examining the substrates that had been brazed we found that, in general, calcium was identified in the spectrum for those samples that had little or no adhesion, but no calcium was in the spectrum for a sample with AD-99 alumina as the substrate and a shear strength with a Ni-Al-Ti-B drop of 137 MPa. Calcium was detected on the surface of samples of both AD-998 and AL-23 alumina after the 1550°C brazing cycle,

but not on the substrates either as received or after the 1000°C thermal treatment. This seems to indicate either that the calcium migrates to the surface (at a level detectable by EDAX) only at temperatures greater than 1000°C (at the 15-min exposure time) or that calcium is being picked up during the braze cycle from the alumina sample boat used. Further study is obviously required to identify the source of the calcium and to either support or refute the idea that this material is responsible for sample-to-sample variability. It would seem likely, however, if calcium is verified as the cause of variability, that the calcium is migrating from within the ceramic substrate rather than coming from an external source. Calcium oxide has a published vapor pressure²⁶ of only 13 μPa (10^{-7} mm Hg) at 2055°C, a temperature much higher than our brazing temperature of 1550°C, and thus transport from an external source is unlikely.

We also examined by EDAX a number of Ni-Al-Ti-B sessile drops as well as unmelted samples of the Ni-Al-Ti-B filler metal used in those tests. As mentioned previously Nicholas and coworkers at Harwell in England have reported major differences in adhesion of sessile drops on both diamond²³ and alumina²⁷ as the composition of the drops was varied over fairly narrow ranges. For example, in a Cu-Ti binary system on diamond, they observed shear strengths of 784 MPa for 0.02 at. % Ti, 186 MPa for Cu-0.05 at. % Ti, but 392 MPa for 0.06 at. % Ti. Although both of these studies dealt with binary systems and with low second-element concentration, they did consistently find that maximum interfacial strengths were produced by alloys with compositions falling within certain very narrow concentration ranges. Thus, in our work, we could have experienced a similar effect if our filler metal were not of uniform composition. Variations in chemistry across a small metal button could occur from insufficient mixing during melting or from solute segregation during solidification.

We did observe instances of anomalous melting behavior in some of the small pieces of filler metal that had been cut from the flattened 1-g buttons or the drop-cast ingots. Such behavior included only partial melting or even no melting at temperatures much above the anticipated liquidus.

We examined the sessile drops from several tests and an unmelted piece of filler metal MWF-21 (Ni-14 Al-10 Ti-0.2 B, at. %) with the EDAX in an effort to determine if there were composition differences. Very close attention was given to procedure, including orientation of each sample with respect to the detector, to obtain X-ray count data that could be compared. The counts detected in a 50-s period are given as ratios for comparison in Table 12. Although this information indicates what appears to be significant differences in composition from one sessile drop to another, there does not seem to be a correlation between these data and adherence behavior of the drops. Note, however, that the Ni/Al and Ti/Al ratios for sample 265 (which had a shear strength of 137 MPa) are clearly lower than those for all of the other samples, all of which had only slight adherence.

Table 12. Energy dispersive X-ray analysis of sessile drops of experimental filler metal MWF-21 (Ni-14 Al-10 Ti-0.2 B, at. %)

Specimen	Ratio of X-ray counts			Remarks
	Ni/Ti	Ni/Al	Ti/Al	
MWF-21	3.89	14.00	3.60	Filler metal as drop cast and homogenized ^a
265	3.63	9.67	2.67	Filler metal had not been homogenized; shear strength = 137 MPa
438	3.29	11.20	3.40	Homogenized filler metal; did not adhere
442	3.16	12.00	3.80	Homogenized filler metal; slight adherence
443	3.20	10.67	3.33	Homogenized filler metal; did not adhere
444	2.70	13.50	5.00	Homogenized filler metal; slight adherence

^aHomogenized in vacuum of 0.8 mPa (6×10^{-6} mm Hg) for 5 h at 1000°C.

EFFECT OF ACTIVE FILLER METALS ON PSZ

Because of an obvious color change produced in the PSZ (see Fig. 7) from contact with molten filler metals containing titanium, we conducted a study to determine if the mechanical properties of the ceramic were also affected. Pieces of filler metal of composition Ag-34 Cu-14 Ti (at. %) were placed on bend bar and DCB specimens of MgO-stabilized PSZ (83-064 MS) as shown in Fig. 21. These samples were brazed in a resistance heated tube furnace for 5 min at 1010°C in a vacuum of about 27 mPa (2×10^{-4} mm Hg). A typical thermal cycle is shown in Fig. 22. The filler metal was then removed by grinding prior to testing. We think the darkening of the PSZ ceramic is attributable to a loss of oxygen from the PSZ into the brazing filler metal. Electron micrographs of brazed samples show a titanium-rich oxide at the filler metal-zirconia interface (Fig. 23). Oxygen is known to be highly mobile in zirconia at temperatures above about 750°C, and X-ray diffraction results from darkened specimens indicated peak broadening that could be explained by a loss of oxygen. The results from our tests (Table 13) indicate that molten active-element-containing filler metals remove enough oxygen from PSZ to cause darkening of this ceramic and some degradation of room temperature strength and toughness.

ORNL-PHOTO 0736-84

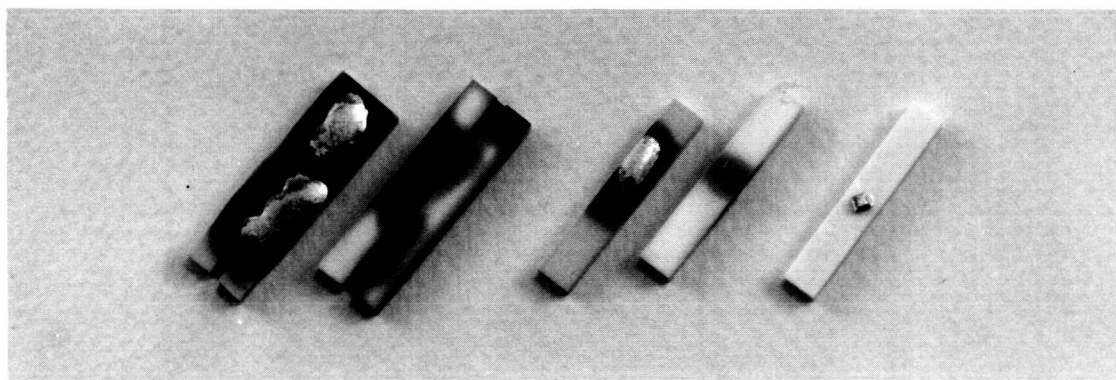


Fig. 21. MgO-stabilized PSZ mechanical property specimens after brazing with Ag-34 Cu-14 Ti, at. %, at 1000°C.

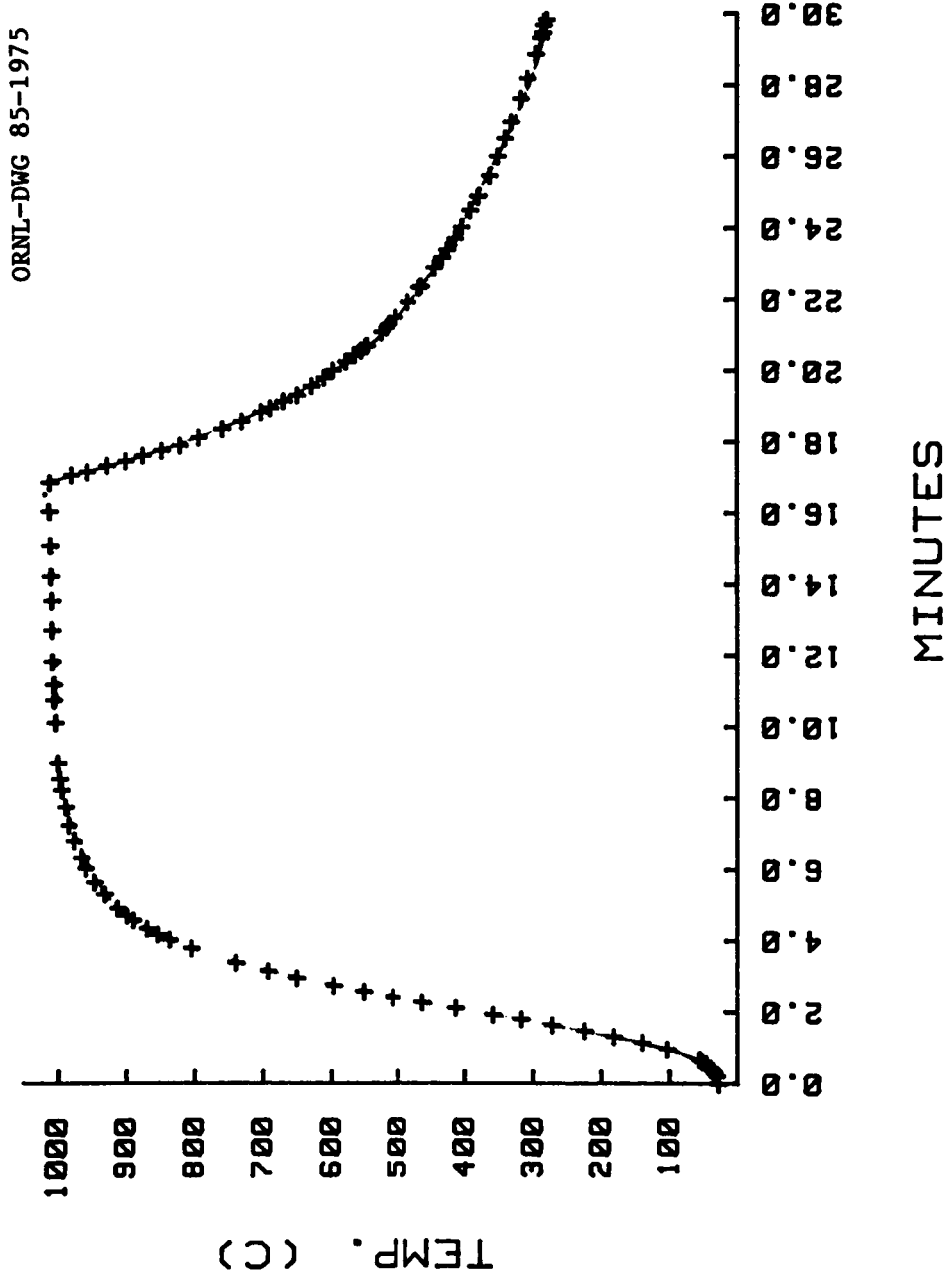


Fig. 22. Typical furnace brazing cycle used in study of the effect of active filler metals on PSZ ceramics.

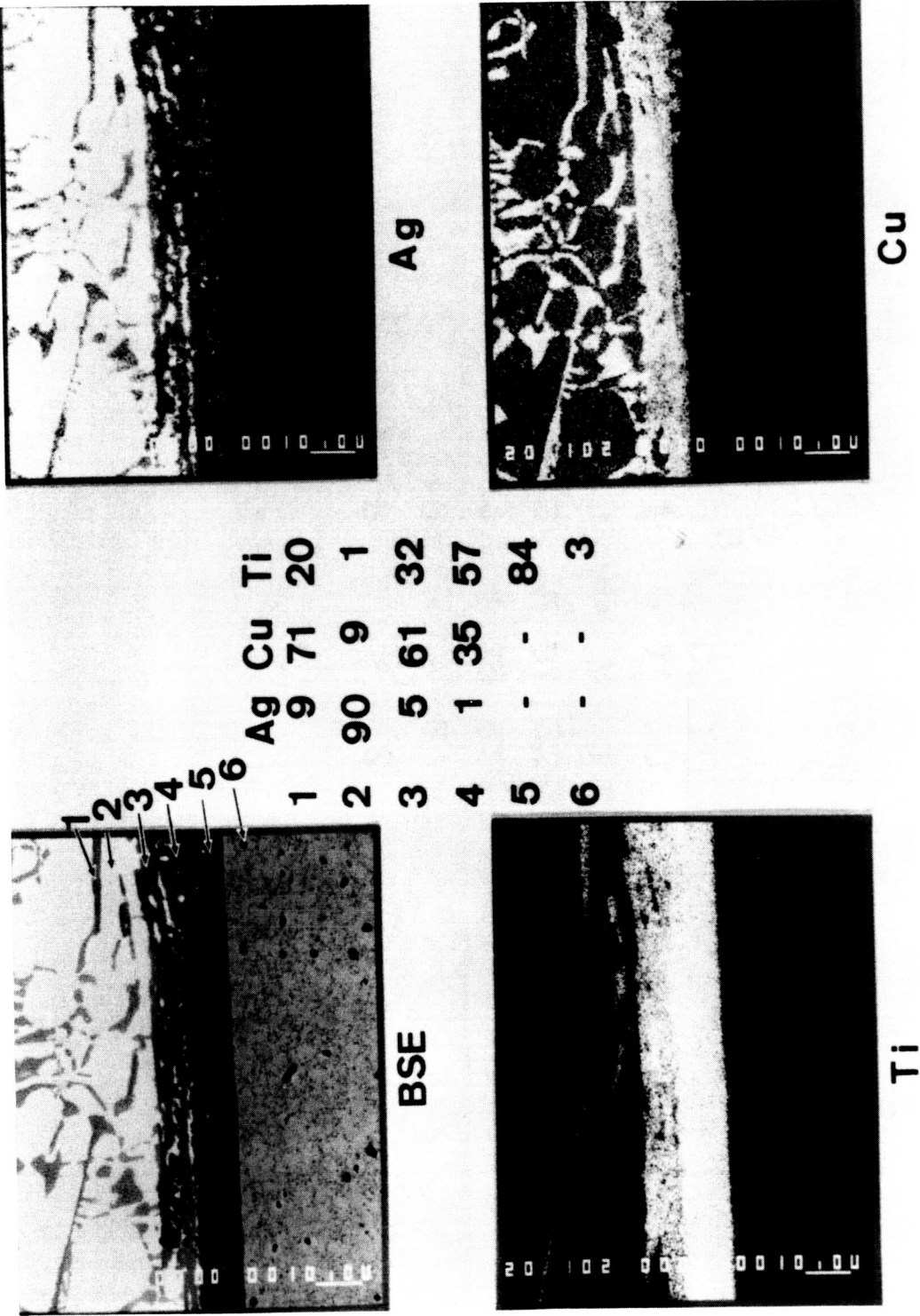


Fig. 23. Back-scattered electron image and elemental concentration displays for TZP ceramic (NGK Z191) brazed with Cu-26 Ag-29 Ti, at. %, at 1000°C. The concentrations indicated are in percent by weight. Note the thick interaction layer at the filler metal-ceramic interface.

Table 13. Comparison of room-temperature mechanical properties of MgO-stabilized PSZ (Nilsen 83-064MS) before and after exposure to a titanium-containing filler metal

	Mean strength ^a (MPa)	Standard deviation	Fracture toughness ^b (MPa·m ^{1/2})	Standard deviation
Before brazing	704	2	14	2
After brazing ^c	652	44	11.5	0.8

^aFour-point bend.

^bApplied moment double cantilever beam.

^cAg-34 Cu-14 Ti, at. %, 5 min at 1010°C, 13 mPa (1 × 10⁻⁴ mm Hg).

COMPARISON OF FILLER METAL WETTING ON MgO- AND Y₂O₃-STABILIZED ZIRCONIAS

A group of six samples, three each of Nilsen's MgO-stabilized material (82-94159N) and NGK's Y₂O₃-stabilized Z-191, were brazed at 1000°C in one batch in a resistance-heated tube furnace with three Cu-Ag-Ti filler metals. The wetting angle of each sessile drop was measured on a shadowgraph after brazing. The results, given in Fig. 24, show that this series of filler metals has slightly poorer wettability on the Y₂O₃-containing ceramic. From a practical brazing standpoint these differences in wetting angle would not be significant. The micrograph (Fig. 25) of one of the sessile drops from this series (CB-142, Cu-26 Ag-29 Ti, at. %, on NGK Z-191 TZP) shows an interfacial layer about 10 μm thick and failure in the PSZ well away from the interface. This type of subsurface cracking has been observed in a number of the sectioned sessile-drop specimens. It is thought to result from a combination of the mismatch in coefficient of thermal expansion between the drop and ceramic substrate and the geometry (and resulting stress state) of the brazement. We have observed that this type of cracking does not occur in this material if the braze joint is configured as a thin film of metal between two pieces of the ceramic, and we assume that the results would be the same for a brazement between the ceramic and a metal having a coefficient of expansion near that of the ceramic.

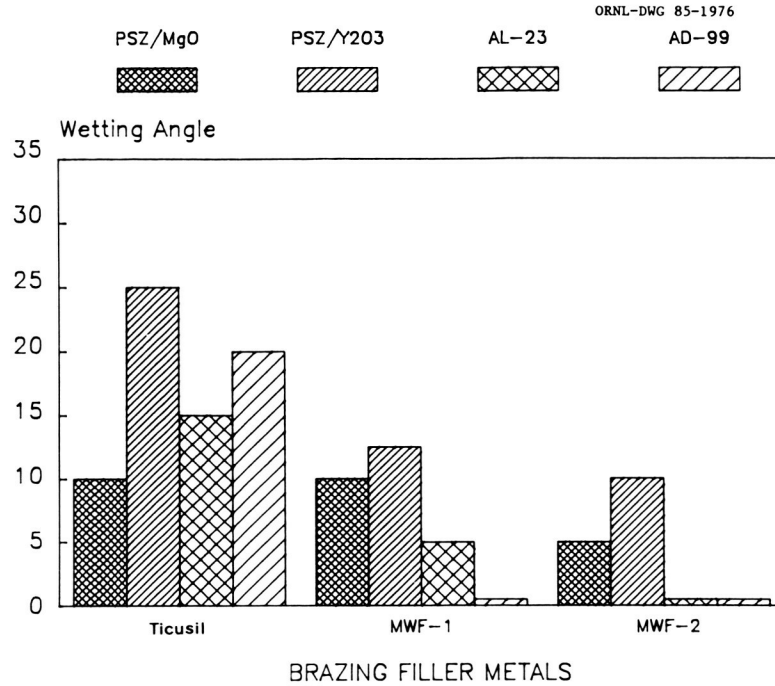


Fig. 24. Wetting behavior on oxide ceramics of a commercial Ag-Cu-Ti filler metal and two of the filler metals studied in this work: MWF-1 (Cu-27 Ag-26 Ti, at. %) and MWF-2 (Cu-26 Ag-29 Ti, at. %). All brazes made at 1000°C in vacuum of 67 mPa (5×10^{-4} mm Hg).



Fig. 25. Cross section of Cu-26 Ag-29 Ti, at. %, sessile drop on NGK Z-191 tetragonal zirconia polycrystalline ceramic. The failure in the ceramic well away from the interface is the result of mismatch in coefficients of thermal expansion but is an indication of the strength of the bond between drop and zirconia.

EFFECT OF 1000°C BRAZING CYCLE ON NODULAR CAST IRON

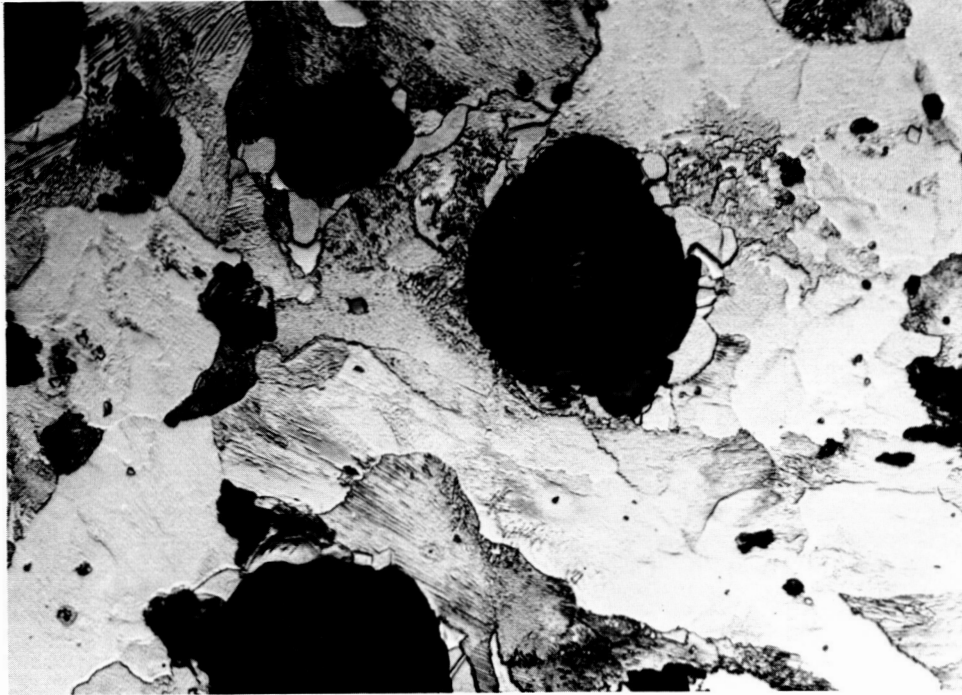
Samples of Izumi nodular cast iron (NCI) that had been exposed to a brazing cycle (Fig. 22) were examined metallographically to determine the effect of the thermal cycle on the microstructure of this piston material.

The 1000°C brazing temperature falls in an "austenite plus graphite" region of the iron-graphite equilibrium diagram. If equilibrium conditions were met, we would expect the original "ferrite plus pearlite plus graphite" structure in the piston material to convert on heating to "austenite plus graphite", which would then retransform on cooling. Because Cummins desires a primarily "pearlite plus graphite" microstructure (on the basis of good high-cycle fatigue strength for this structure), we were interested in the structure following a typical brazing cycle. In this cycle, the cooling rate was 150°C/min down to 750°C (near the lower transformation temperature for NCI) and a slower rate below 750°. We were pleased to find that the hardness of the iron after brazing was about the same as before brazing ($R_B = 100$) and that the microstructures were similar as can be seen in Fig. 26. Note that the graphite nodules are somewhat smaller in the NCI after the brazing cycle, but that the basic microstructure still consists of ferrite plus pearlite (with possibly some upper bainite). These results indicate that metallurgically it would be feasible to directly braze PSZ to NCI at a temperature as high as 1000°C. However, such an operation might not be desirable from a thermal expansion mismatch standpoint, so it still may be best to use a transition material in this brazement.

SUMMARY AND CONCLUSIONS

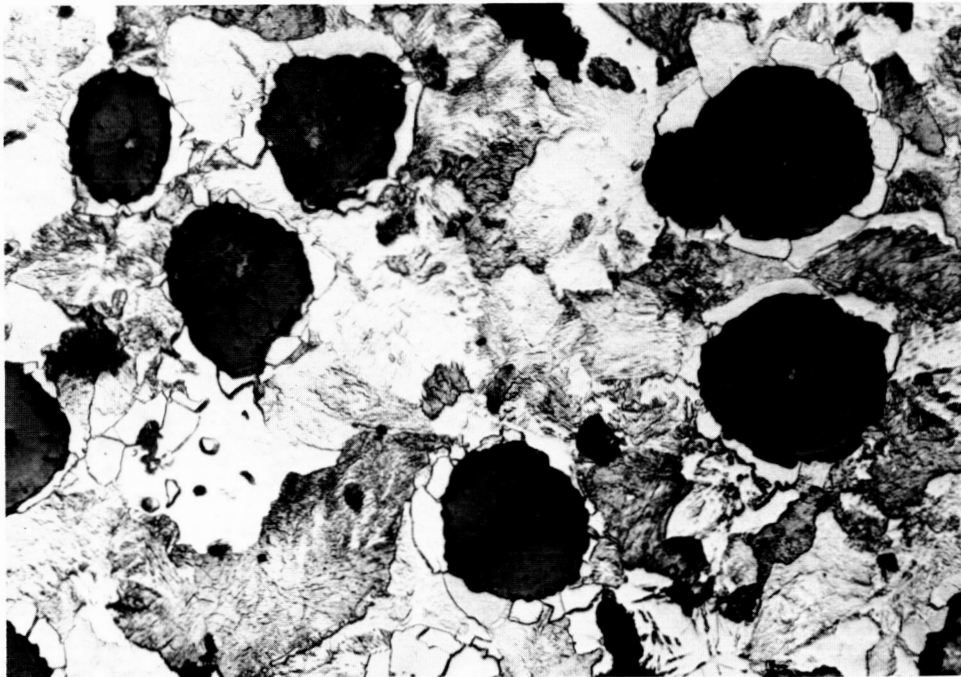
The wetting and adherence behavior in vacuum of a series of metal alloys on structural ceramics including high-purity aluminas, partially stabilized zirconias, and a SiC-whisker-reinforced alumina-matrix composite was investigated. Wetting was determined through measurement of the contact angle of solidified sessile drops. Adherence was measured at room temperature by shearing off the sessile drops and by four-point flexure tests of ceramic-ceramic specimens brazed in a butt configuration.

Y-198880



(a)

Y-198878



(b)

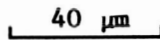
40 μm

Fig. 26. Nodular cast iron (Izumi) piston material. (a) As received. (b) After 5 min at 1000°C braze cycle. Etchant, 2% Nital.

Flexural tests were also conducted in air at temperatures up to 600°C. The fracture toughness of some specimens was determined through use of a composite applied moment double cantilever beam specimen developed in this work. Finally the shear strength of ceramic-metal brazements was measured using a bar/pad shear specimen developed at Oak Ridge National Laboratory. Significant conclusions from this work include:

1. Of the series of alloys studied that were based on the Ag-Cu eutectic with additions of Ni and Ti, the best results were achieved with the Cu-26 Ag-29 Ti, at. %, composition. This filler metal produced wetting angles less than 30° on all the ceramics, and flexural strengths at 400°C greater than 165 MPa for alumina and greater than 130 MPa for a PSZ brazement.
2. Of the gold-bearing filler metals, the Cu-20 Au-18 Ti, at. %, had superior properties. Flexural strengths at 400°C of brazements made with this filler metal ranged from 106 MPa for AL-23 alumina to 218 MPa for AD-998 alumina. The room-temperature flexural strength of PSZ brazed with this material was 258 MPa.
3. The fracture toughness of composite specimens of PSZ brazed with the Cu-27 Ag-26 Ti, at. %, filler metal averaged about the same as that of the bulk ceramic, 6 MPa·m^{1/2}.
4. Some excellent (>200 MPa) shear strengths were obtained in Cu-26 Ag-29 Ti, at. %, brazements between NCI and PSZ or between type 446 stainless steel and PSZ. However, there was a subset of data with shear strengths of only about 25 MPa. No reason was found for this variability.
5. Active-element-containing alloys produce a darkening of PSZ ceramics, and a modest decrease in the strength and toughness of a MgO-stabilized PSZ ceramic after exposure to a molten filler metal.
6. There was slightly poorer wetting (greater wetting angle) of the Cu-Ag-Ti filler metals on tetragonal zirconia polycrystalline (TZP) ceramic stabilized with Y₂O₃ than on MgO-stabilized PSZ material. However, from a practical brazing standpoint these differences in wetting behavior would not be significant.

7. A brazing cycle to 1000°C did not harm either the hardness or microstructure of a NCI piston material. These data indicate that the brazing temperature for joints including this alloy does not have to be limited to less than 750°C.

REFERENCES

1. L. Reed, "Ceramic to Metal Sealing," *Electronic Ceramics*, Special Publication No. 3, American Ceramic Society, Columbus, Ohio, 1969.
2. W. H. Kohl, *Handbook of Materials and Techniques for Vacuum Devices*, Reinhold, New York, 1967, pp. 451-52, 455-56.
3. D. M. Mattox, "Metallizing Ceramics Using a Gas Discharge," *J. Am. Ceram. Soc.* **38**(7), 385-86 (1965).
4. R. L. Bronnes et al., "Ceramic-to-Metal Bonding with Sputtering as a Metallization Technique," *Philips Tech. Rev.* **35**(7-8), 209-11 (1975).
5. C. W. Fox and G. M. Slaughter, "Brazing of Ceramics," *Weld. J. (N.Y.)* **43**(7), 591-97 (1964).
6. D. A. Canonico et al., "Direct Brazing of Ceramics, Graphite and Refractory Metals," *Weld. J. (Miami)* **56**(8), 31-38 (1977).
7. G. C. Wei and P. F. Becher, "Development of SiC-Whisker-Reinforced Ceramics," *Am. Ceram. Soc. Bull.* **64**(2), 298-304 (1985).
8. B. C. Allen and W. D. Kingery, "Surface Tension and Contact Angles in Some Liquid Metal-Solid Ceramic Systems at Elevated Temperatures," *Trans. Metall. Soc. AIME* **215**(2), 30-36 (1959).
9. L. E. Murr, "Interfacial Energetics in Metal-Metal, Metal-Ceramic, Metal-Semiconductor, and Related Solid-Solid and Liquid-Solid Systems," in *Interfacial Phenomena in Metals and Alloys*, L. E. Murr editor, Addison-Wesley Publishing Co., Inc., Reading, Mass., 1975.
10. J. E. Ritter, Jr., and M. S. Burton, "Adherence and Wettability of Nickel, Nickel-Titanium Alloys, and Nickel-Chromium Alloys to Sapphire," *Trans. Metall. Soc. AIME* **239**, 21-26 (Jan. 1967).
11. H. T. Corten, *Fracture*, Vol. VII, H. Liebowitz, ed., Academic Press, New York, 1972, pp. 676-769.

12. D. R. Mulville and R. H. Vaishnav, *Proceedings of Symposium on Solid Mechanics*, AMMRC MS-74-81, Army Materials and Mechanics Research Center, Watertown, Mass., 1974.
13. J. R. Rice and G. C. Sih, *J. Appl. Mech., Ser. E*, **32**(2), 418-23 (1965).
14. E. Wu and R. L. Thomas, "Interfacial Fracture Phenomena," in *Proceedings of the Fifth International Congress on Rheology*, Vol. 1, S. Onogi, ed., University Park Press, Baltimore, 1969.
15. G. Elssner and R. Pabst, "Mechanical Properties of Ceramics," R. W. Davidge, ed., in *Proc. Brit. Ceram. Soc.* **25**, 179-86 (1975).
16. W. D. Bascom et al., "Use of Fracture Mechanics Concepts in Testing of Film Adhesion," pp. 63-81 in *Proceedings of the ASTM Symposium on Adhesion Measurement of Thin Films, Thick Films, and Bulk Coatings*, ASTM-STP640, K. L. Mittal, ed., American Society for Testing and Materials, Philadelphia, 1978.
17. P. F. Becher and S. A. Halen, in "Ceramics for High Performance Applications-II," *Proceedings of the Fifth Army Materials Technology Conference, Newport, R.I., March 21-25, 1977*, J. J. Burke, E. N. Leno, and R. N. Katz, eds., Brook Hill Publishing Co., Chestnut Hill, Mass., 1978.
18. W. H. Sutton, "Wetting and Adherence of Ni/Ni-Alloys to Sapphire," presented at 66th Annual Meeting, American Ceramic Society, Chicago, April 22, 1964.
19. M. Nicholas, R. R. D. Forgan, and D. M. Poole, "The Adhesion of Metal/Alumina Interfaces," *J. Mater. Sci.* **3**, 9-14 (1968).
20. V. J. Tennery et al., "Characterization of the Fatigue and Slow Crack Growth Behavior of Partially Stabilized Zirconia Ceramics," pp. 409-18 in *Proceedings of the 22nd Automotive Technology Development Contractors' Coordination Meeting*, P-155, Society of Automotive Engineers, Inc., Warrendale, Pa., March 1985.
21. G. Economos and W. D. Kingery, "Metal-Ceramic Interactions: II, Metal-Oxide Interfacial Reactions at Elevated Temperatures," *J. Am. Ceram. Soc.* **36**(12), 403-9 (1953).
22. M. Hansen, *Constitution of Binary Alloys*, McGraw-Hill Book Co., New York, 1958, p. 1069.

23. D. Evens, M. Nicholas, and P. M. Scott, "The Wetting and Bonding of Diamonds by Copper-Tin-Titanium Alloys," *Ind. Diamond Rev.* 306-9, (September 1977).

24. P. F. Becher and J. S. Murday, "Thick Film Adherence Fracture Energy: Influence of Alumina Substrates," *J. Mater. Sci.* 12, 1088-94 (1977).

25. S. K. Rhee, "Wetting of Ceramics by Liquid Metals," *J. Am. Ceram. Soc.* 54(7), 332-34 (1971).

26. P. T. B. Shaffer, *High Temperature Materials No. 1 - Materials Index*, Plenum Press, New York, 1964, p. 326.

27. M. Nicholas, "The Strength of Alumina-Metal Alloy Interfaces," *Sci. Ceram.* 5, 377-91 (1970).

DOE/NASA/4148-1
 NASA CR-175019
 ORNL-6262
 Dist. Category UC-95

INTERNAL DISTRIBUTION

- | | | | |
|--------|-------------------------------|--------|-----------------------------|
| 1-2. | Central Research Library | 30. | C. J. McHargue |
| 3. | Document Reference Section | 31-35. | A. J. Moorhead |
| 4-5. | Laboratory Records Department | 36. | R. K. Nanstad |
| 6. | Laboratory Records, ORNL RC | 37. | M. L. Santella |
| 7. | ORNL Patent Section | 38. | A. C. Schaffhauser |
| 8. | P. F. Becher | 39. | J. L. Scott |
| 9. | R. A. Bradley | 40. | G. M. Slaughter |
| 10. | A. J. Caputo | 41. | J. O. Stiegler |
| 11. | R. S. Carlsmith | 42. | D. P. Stinton |
| 12. | J. A. Carpenter, Jr. | 43. | V. J. Tennery |
| 13. | F. C. Chen | 44-46. | P. T. Thornton |
| 14. | R. M. Davis | 47. | T. N. Tiegs |
| 15. | J. I. Federer | 48. | J. M. Vitek |
| 16. | B. E. Foster | 49. | C. L. White |
| 17. | R. L. Graves | 50. | R. O. Williams |
| 18. | R. L. Heestand | 51. | A. Zucker |
| 19. | D. R. Johnson | 52. | R. J. Charles (Consultant) |
| 20. | R. R. Judkins | 53. | G. Y. Chin (Consultant) |
| 21-25. | H. Keating | 54. | H. E. Cook (Consultant) |
| 26. | J. F. King | 55. | Alan Lawley (Consultant) |
| 27. | E. L. Long, Jr. | 56. | W. D. Nix (Consultant) |
| 28. | R. W. McClung | 57. | J. C. Williams (Consultant) |
| 29. | R. N. McGill | | |

EXTERNAL DISTRIBUTION

58. ADIABATICS, INC., 630 S. Mapleton, Columbus, IN 47201
 R. Kamo
59. AEROSPACE CORPORATION, 2350 East El Segundo Blvd.,
 El Segundo, CA 90009
 W. U. Roessler
60. ALLISON GAS TURBINE OPERATIONS, P.O. Box 420, Indianapolis, IN
 46206-0420
 D. L. Clingman
61. AMERICAN TRUCKING ASSOCIATIONS, INC., 2200 Mill Road,
 Alexandria, VA 22314
 V. Suski

62. APPLICATION COMPANY, LTD., Analysis & Design, 60 Broadhollow Road, Melville, NY 11747
P. S. MacDonald
63. ARGONNE NATIONAL LABORATORY, 9700 South Cass Avenue, Argonne, IL 60439
Robert Holtz
64. ARMY MATERIALS AND MECHANICS RESEARCH CENTER, Arsenal Street, Watertown, MA 02172
R. N. Katz
65. ARO, P.O. Box 12211, Research Triangle Park, NC 27709
David Mann
66. BARBER NICHOLS ENGINEERING, 6365 W. 55th Street, Arvada, CO 80002
R. Barber
67. BATTELLE PACIFIC NORTHWEST LABORATORIES, 2030 M Street NW, Washington, DC 20036
J. C. Franke
68. BATTELLE PACIFIC NORTHWEST LABORATORIES, P.O. Box 999, Richland, WA 99352
Paul Koehnstead
69. CARBORUNDUM COMPANY, P.O. Box 832, Niagara Falls, NY 14302
R. Storm
70. CATERPILLAR TRACTOR COMPANY, Research Department, Technical Center, Peoria, IL 61629
J. M. Bailey
71. CHRYSLER CORPORATION, P.O. Box 1118, Detroit, MI 48288
L. B. Mann
72. CONCEPT ANALYSIS CORPORATION, 9145 General Court, Plymouth, MI 48170
P. C. Glance
73. COORS PORCELAIN COMPANY, Director, Technical Operations, 17750 N. 32nd St., Golden, CO 80401
D. G. Wirth
74. CUMMINS ENGINE COMPANY, INC., P.O. Box 3005, Columbus, IN 47201
Michael Brands

75. JOHN DEERE AND COMPANY, John Deere Road, Moline, IL 61265
J. D. Spuller
- 76-77. DETROIT DIESEL ALLISON, Speed Code R03B, 36880 Ecorse Road,
Romulus, MI 48239-4001
Nabil Hakim
R. B. Wallace
78. DRESSER INDUSTRIES, Waukesha Engine Division, P.O. Box 379,
Waukesha, WI 53167
W. E. Snyder
79. EATON CORPORATION, Engine and Research Center, 26201 Northwestern
Highway, P.O. Box 766, Southfield, MI 48037
Richard Chute
80. E-F TECHNICAL ASSOCIATES, P.O. Box 189, St. Johns, MI 48879
R. R. Tison
81. ETHYL CORPORATION, 451 Florida Street, Baton Rouge, LA 70801
Michael Dubeck
82. FORD MOTOR COMPANY, P.O. Box 2053, Dearborn, MI 48121
Wally Wade
83. FREIGHTLINER CORPORATION, R&D, 4747 N. Channel Avenue,
P.O. Box 4849, Portland, OR 97208
R. Murphy
84. GA TECHNOLOGIES, INC., P.O. Box 81608, San Diego, CA 92138
F. Warner
85. GARRETT CORPORATION, One First National Plaza, Suite 1900,
Dayton, OH 45402
A. E. Hause
86. GARRETT TURBINE ENGINE COMPANY, P.O. Box 5217, Phoenix, AZ 85010
Jere Castor
- 87-88. GENERAL ELECTRIC COMPANY, Bldg. 7, Advanced Energy Program
Department, P.O. Box 527, King of Prussia, PA 19406
J. A. Bledsoe
S. Musikant
89. GENERAL MOTORS CORPORATION, Electromotive Division, La Grange, IL
60525
N. R. Dunteman

- 90-92. GENERAL MOTORS RESEARCH LABORATORIES/TECHNICAL CENTER,
Engine Research Department, Warren, MI 48090
A. C. Alkidas
Chuck Amann
David Dimick
93. W. R. GRACE AND COMPANY, 7379 Route 32, Columbia, MD 21044
Roy Rice
94. GTE LABORATORIES INCORPORATED, 40 Sylvan Road, Waltham, MA 02254
C. O. Dugger
95. HOWMET TURBINE COMPONENTS CORPORATION, 1600 Warner Road,
Whitehall, MI 49461
L. G. McCoy
96. HQDA (DAMA-ARA), Washington, DC 20310
Charles Church
97. IMPERIAL CLEVITE, INC., Technology Center, 540 E. 105th Street,
Cleveland, OH 44108
Technical Library
98. INTEGRAL TECHNOLOGIES, INC., 415 E. Plaza Drive, Westmont, IL
60559
99. JET PROPULSION LABORATORY, 4800 Oak Grove Drive, Pasadena, CA
91103
M. Dowty
100. KOHLER COMPANY, 444 Highland Drive, Kohler, WI 53044
James McCandless
101. A. D. LITTLE, INC., Acorn Park, Cambridge, MA 02140
R. G. Colello
102. MACK TRUCKS, INC., Box M, Allendale, PA 18105
F. J. Pekar
- 103-104. MASSACHUSETTS INSTITUTE OF TECHNOLOGY, Department of Mechanical
Engineering, Cambridge, MA 02139
J. Ekchian
J. B Heywood
105. MECHANICAL TECHNOLOGY INC., 968 Albany-Shaker Road, Latham, NY
12110
Wilbur Shapiro

106. MERIDIAN CORPORATION, 5113 Leesburg Pike, Suite 700,
Falls Church, VA 22041
S. J. Goguen
107. MUELLER ASSOCIATES, 1401 South Edgewood Street, Baltimore, MD
21227
T. Timbario
- 108-109. NASA HEADQUARTERS, Washington, DC 20546
John Facey
- 110-125. NASA, Lewis Research Center, 21000 Brookpark Road,
Cleveland, OH 44135
Library, M.S. 60-3 (2 copies)
Patent Counsel, M.S. 60-2
Report Control, M.S. 60-1
M. Bailey, 77-6
R. Barrows, 77-6
R. Evans, 77-6
G. Reck, 86-1
W. Sanders, 49-3
H. Sliney, 23-2
T. Strom, 77-6
W. Wintucky, 77-6
E. Willis, 77-6
J. Wood, 77-6
H. Yacobucci, 77-6
J. Ziemianski, 86-1
- 126-150. NASA SCIENTIFIC & TECHNICAL INFORMATION FACILITY, P.O. Box 8757,
Baltimore/Washington International Airport, MD 21240
Accessioning Department
151. NAVISTAR INTERNATIONAL, 10400 W. North Avenue, Melrose Park,
IL 60160
William Lenzi
152. NAVSEA, 1000 Jefferson Davis Highway, Washington, DC 20007
D. Groghan
153. NORTON COMPANY, 1 New Bond Street, Worcester, MA 01606
K. Subramanian
154. PACCAR INC., Business Center Building, P.O. Box 1518, Bellevue, WA
98009
J. M. Dunn

155. LOUIS PECK AND ASSOCIATES, Box 212, Pittsford, NY 14534
156. PERKINS ENGINES, INC., 24175 Research Drive, Farmington, MI 48024
Engineering Department
157. RAMSEY CORPORATION, 1233 Manchester Road, Manchester, MO 63011
H. E. McCormick
158. RICHARDO CONSULTING ENGINEERS, LTD., Bridge Works, Shoreham-by-Sea,
Sussex, BN45FG, ENGLAND
S. R. Norris-Jones
159. SANDIA NATIONAL LABORATORIES, Combustion Applications Division,
Livermore, CA 94550
Michal Dyer
160. SKF INDUSTRIES, INC., SKF Technology Services, P.O. Box 515,
King of Prussia, PA 19406
P. A. Madden
161. SOUTHWEST RESEARCH INSTITUTE, Department of Material Sciences,
P.O. Drawer 28570, 6220 Culebra Drive, San Antonio, TX 78284
James Lankford
162. SUNDSTRAND ENERGY SYSTEMS, 4747 Harrison Avenue, Rockford, IL
61101
D. Lacey
163. SVERDRUP TECHNOLOGY, INC., P.O. Box 30650 Midpark Branch,
Middleburg Heights, OH 44130
R. G. Ragsdale
164. TELEDYNE CONTINENTAL, 76 Getty Street, Muskegon, MI 49442
S. G. Berenyl
165. THERMO ELECTRON CORPORATION, 101 First Avenue, Waltham, MA 02154
Michael Koplw
166. TIMONEY RESEARCH LIMITED, Dublin Road, Trim Co., Meath, IRELAND
S. G. Timoney
167. TRW, INC., 1455 East 185 Street, Cleveland, OH 44110
R. R. Wills
168. U.S. ARMY TANK AUTOMOTIVE COMMAND AND DEVELOPMENT CENTER,
Warren, MI 48090
W. Brysik (DRSTA/RGED)

169. U.S. MARITIME ADMINISTRATION, Room 7330, Code MAR-760,
400 7th Street, SW, Washington, DC 20590
Frank Crotelli
170. UNITED TECHNOLOGIES RESEARCH CENTER, Silver Lane, East Hartford,
CT 06108
G. S. Hausmann
171. WESTINGHOUSE ELECTRIC CORPORATION, R&D Center, 1310 Beulah Road,
Pittsburgh, PA 15235
D. J. Boes
172. WHITE ENGINES, INC., Canton, OH 44707
E. J. Caruso
- 173-185. DOE, CONSERVATION AND RENEWABLE ENERGY, Forrestal
Building, Washington, DC 20585
J. J. Eberhardt, CE-14
John Fairbanks, CE-131 (10 copies)
M. E. Gunn, CE-14
T. M. Levinson, CE-14
186. DOE, MORGANTOWN ENERGY TECHNOLOGY CENTER, P.O. Box 880,
Morgantown, WV 26505
L. K. Carpenter
187. DOE, OAK RIDGE OPERATIONS OFFICE, P.O. Box E, Oak Ridge, TN 37831
Office of Assistant Manager for Energy Research and Development
- 188-339. DOE, TECHNICAL INFORMATION CENTER, Office of Information Services,
P.O. Box 62, Oak Ridge, TN 37831

For distribution by microfiche as shown in DOE/TIC-4500,
Distribution Category UC-95 (Energy Conservation)